

The Plant Journal (2023) 116, 478-496

doi: 10.1111/tpj.16385

The regulation of chromatin configuration at *AGAMOUS* locus by LFR-SYD-containing complex is critical for reproductive organ development in Arabidopsis

Xiaowei Lin^{1,2,†,*}, Tingting Yuan^{1,†,‡}, Hong Guo¹, Yi Guo¹, Nobutoshi Yamaguchi³, Shuge Wang¹, Dongxia Zhang¹, Dongmei Qi^{1,§}, Jiayu Li¹, Qiang Chen¹, Xinye Liu¹, Long Zhao⁴, Jun Xiao⁴, Doris Wagner⁵, Sujuan Cui^{1,*} and Hongtao Zhao^{1,*}

¹Hebei Key Laboratory of Molecular and Cellular Biology, Key Laboratory of Molecular and Cellular Biology of Ministry of Education, Hebei Research Center of the Basic Discipline of Cell Biology, Hebei Collaboration Innovation Center for Cell Signaling, College of Life Science, Hebei Normal University, Shijiazhuang 050024, China,

Received 9 December 2022; revised 28 May 2023; accepted 27 June 2023; published online 21 July 2023.

SUMMARY

Switch defective/sucrose non-fermentable SWI/SNF) chromatin remodeling complexes are evolutionarily conserved, multi-subunit machinery that play vital roles in the regulation of gene expression by controlling nucleosome positioning and occupancy. However, little is known about the subunit composition of SPLAYED SYD)-containing SWI/SNF complexes in plants. Here, we show that the Arabidopsis thaliana Leaf and Flower Related LFR) is a subunit of SYD-containing SWI/SNF complexes. LFR interacts directly with multiple SWI/SNF subunits, including the catalytic ATPase subunit SYD, in vitro and in vivo. Phenotypic analyses of Ifr 2 mutant flowers revealed that LFR is important for proper filament and pistil development, resembling the function of SYD. Transcriptome profiling revealed that LFR and SYD shared a subset of coregulated genes. We further demonstrate that the LFR and SYD interdependently activate the transcription of AGAMOUS AG), a C-class floral organ identity gene, by regulating the occupation of nucleosome, chromatin loop, histone modification, and Pol II enrichment on the AG locus. Furthermore, the chromosome conformation capture 3C) assay revealed that the gene loop at AG locus is negatively correlated with the AG expression level, and LFR-SYD was functional to demolish the AG chromatin loop to promote its transcription. Collectively, these results provide insight into the molecular mechanism of the Arabidopsis SYD-SWI/SNF complex in the control of higher chromatin conformation of the floral identity gene essential to plant reproductive organ development.

Keywords: Arabidopsis, LFR, SWI/SNF, SYD, AG, filament, pistil.

INTRODUCTION

In eukaryotes, gene transcriptional activity is precisely controlled by dynamic changes in chromatin accessibility in response to developmental and environmental signals (Ramirez-Prado & Benhamed, 2021). Switch defective/sucrose non-fermentable (SWI/SNF) chromatin remodeling complexes are crucial for mediating these chromatin changes by utilizing energy from ATP hydrolysis to regulate nucleosome occupation and positioning (Wagner, 2003;

Xiao, Jin, & Wagner, 2017). SWI/SNF complexes are multi-subunit machinery, evolutionarily conserved among yeasts, animals, and plants (Clapier & Cairns, 2009; Han et al., 2015; Ramirez-Prado & Benhamed, 2021). According to sequence similarity with known SWI/SNF components of other eukaryotes, four Snf2-type ATPases of SWI/SNF complexes were identified in the Arabidopsis genome, including BRAHMA (BRM), plant-specific SWI/SNF ATPases SPLAYED (SYD), MINUSCULE 1 and 2 (MINU1 and 2, also

²School of Traditional Chinese Medicine, Tianjin University of Traditional Chinese Medicine, Tianjin 301617, China,

³Biological Science, Nara Institute of Science and Technology, 8916-5, Takayama, Ikoma, Nara 630-0192, Japan,

⁴Institute of Genetics and Developmental Biology, Chinese Academy of Sciences, Beijing, China,

⁵Department of Biology, University of Pennsylvania, Philadelphia 19104-6084, Pennsylvania, USA

For correspondence (e-mail linxiaoweiwqhz@163.com, cuisujuan@hebtu.edu.cn, zhaohongtao@hebtu.edu.cn).

[†]These authors contributed equally to this work.

[‡]Present address: Department of Biology, Arrowhead Pharmaceuticals, 502 South Rosa Road, Madison, Wisconsin 53719, USA

[§]Present address: College of Biological and Food Science, Hebei Normal University for Nationalities, Chengde 067000, China

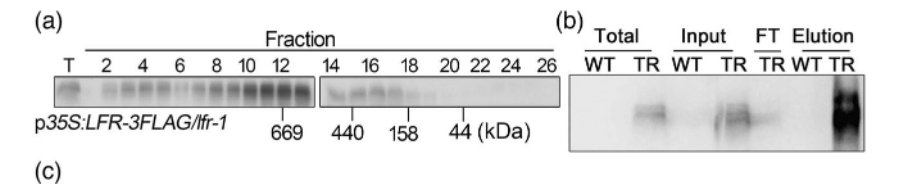
known as CHR12 and 23) (Farrona et al., 2004; Hurtado et al., 2006; Mlynarova et al., 2007; Sang et al., 2012; Su et al., 2006; Wagner & Meyerowitz, 2002). In addition to the core catalyzing enzyme, several other subunits were also identified according to sequence homology with known SWI/SNF components of other eukaryotes, including the single SNF5 subunit termed BUSHY (BSH), four SWI3 proteins (SWI3A SWI3D), two SWI/SNF associated proteins 73 (SWP73A) and SWP73B (also known as CHCs or BAF60s), in addition to two actin-related proteins (ARP4) and ARP7 (Brzeski et al., 1999; Han et al., 2015; Jerzmanowski, 2007; Reyes, 2014; Sarnowska et al., 2016; Sarnowski et al., 2005). Different SWI/SNF subunits enable the combinatorial assembly of variant forms of complexes with distinct properties (Ramirez-Prado & Benhamed, 2021). A typical, canonical, plant SWI/SNF complex is thought to contain one ATPase, one SNF subunit, two SWI3 subunits, and one SWP73 (Han et al., 2015). These core catalytic enzymes and other SWI/SNF components are involved in plant vegetative and reproductive organ development, phase transition, as well as responses to hormone and environmental stimuli through the transcriptional control of relevant target genes by varying genome accessibility in plants (Bezhani et al., 2007; Reyes, 2014; Sarnowska et al., 2016; Shang & He, 2022). A series of informative genome-wide occupancy analyses of SWI/SNF subunits (BRM, SYD, and BAF60) by chromatin immunoprecipitation-sequencing (ChIP-seq), combined with transcriptome profiling revealed their similar enrichment patterns, acting as both activators and repressors of gene expression (Archacki et al., 2017; Jegu et al., 2017; Li et al., 2016; Shu et al., 2021). Furthermore, immunoprecipitation combined with mass spectrometry (IP-MS) were used to efficiently identify new core subunits of SWI/SNF, namely: two BRM interacting protein (BRIP1 and BRIP2), three bromodomain-containing proteins (BRD1, BRD2, and BRD13), and two TRIPLE PHD FINGERS proteins (TPF1 and TPF2) (Hernandez-Garcia et al., 2022; Jaronczyk et al., 2021; Ramirez-Prado & Benhamed, 2021; Yu et al., 2020, 2021), which greatly improved collective understanding in the composition of plant BRM- and MINU-containing SWI/SNF complex; however, the plant SYD-containing complex remains poorly elucidated.

Most angiosperm flowers are organized into four concentric whorls, for example, Arabidopsis flowers have four sepals, four petals, six stamens (the male reproductive organs), and two fused carpels (pistil, the female reproductive organs). Stamens and pistils form in almost all angiosperm flowers and are pivotal for both reproductive success and survival (Litt & Kramer, 2010). Floral organ identity is specified by the four classes of homeotic regulators termed ABCE, among which class B and C genes specify stamen and pistil identity. *AGAMOUS* (*AG*) is the only C-class gene function in the male and female reproductive organs and contributes to flower meristem determinacy

(Bowman et al., 1991; Dennis & Peacock, 2019; Ito et al., 2004; Krizek & Fletcher, 2005; Liu et al., 2014; Yanofsky et al., 1990). SWI/SNF complex components were reported to affect flower development: SWI/SNF chromatin remodeling ATPases are recruited by the MONOPTEROS transcription factor to the chromatin for key regulators of flower primordium initiation, directly increasing accessibility of their genomic DNA (Wu et al., 2015). Furthermore, SYD and BRM play redundant roles in flower patterning by directly activating the expression of APETALA3 (AP3, class B gene) and AG, counteracting the repressive effects mediated by the Polycomb Repressive Complex 2 (PRC2) (Wu et al., 2012). In addition, SWP73B plays an important role in flower development by directly changing the nucleosome occupancy, and promoting the transcriptional expression level of the key floral identity genes, such as APETALA1 (AP1, class A gene), AP3, and SEPALLATA3 (SEP3, class E gene) (Sacharowski et al., 2015). SWP73B is also involved in the chromatin loop formation of the FLOWERING LOCUSC (FLC) gene, a flowering repressor belonging to the MADS-box family (Jegu et al., 2014). The floral homeotic gene AG also encodes a MADS-box transcription factor, and has a 3-kb second intron in the AG gene, which is key to the appropriate spatiotemporal expression of this gene for regulating floral cell fate decisions and maximizing reproductive fitness (Pelayo et al., 2021). Intriguingly, AG is regulated by multi-layered epigenetic mechanisms, such as noncoding RNA (Wu et al., 2018), histone modification (Pelayo et al., 2021), and histone variant (Lee et al., 2022); however, the higher-order chromatin structure at this locus remains unclear (Ramirez-Prado & Benhamed, 2021).

Leaf and Flower Related (LFR) was predicted to encode a nuclear Armadillo (ARM)-repeat protein (Wang et al., 2009). Notably, LFR depletion resulted in defects in leaf and flower development (Wang et al., 2009). Our previous studies have shown that LFR directly interacts with AS2 or SWI3B to control the expression of BREVIPEDICEL-LUS (BP) or FILAMENTOUS FLOWER (FIL) and IAA carboxyl methyltransferase 1 (IAMT1), respectively, during leaf development (Lin et al., 2018, 2021). Although the molecular mechanism of LFR in leaf development has been deciphered, its detailed function in flower development is largely unknown. LFR was identified in the IP-MS complex of AN3 and SWP73B (Nelissen et al., 2015; Vercruyssen et al., 2014); however, whether Arabidopsis LFR stably exists in the SWI/SNF complex, as well as the physical and genetic interactions between LFR and SWI/SNF ATPase, remain largely unknown.

Here, we show that LFR is involved in the SYD-containing SWI/SNF complex in Arabidopsis. We found that LFR physically interacts with SWI/SNF complex components, including the ATPase SYD, in vivo and in vitro. The N-terminus of SYD, including the QLQ domain, is



Locus name	ID Protein	Peptides	MW (kDa)
AT3G22990	LFR	39	50
AT2G28290	SYD	80	387(180)
AT4G34430	SWI3D	52	108
AT5G14170	SWP73B	40	59
AT1G18450	ARP4	62	49
AT3G60830	ARP7	10	40
AT5G07940	SYS1	11	168.9
AT5G07970	SYS2	18	121.1
AT5G07980	SYS3	29	164.3
AT3G18780	ACTIN2	138	41.9
AT5G09810	ACTIN7	32	41.7
AT4G22320	BCL7A	8	26.3
AT5G55210	BCL7B	22	18.5
AT3G06010	MINU1	69	130
AT5G19310	MINU2	20	128
AT2G47620	SWI3A	78	57
AT2G33610	SWI3B	9	52
AT3G01890	SWP73A	1	51
AT3G17590	BSH	1	27
AT1G58025	BRD5	33	86.5
AT3G52100	TPF1	12	77.4
AT3G08020	TPF2	11	86.2
AT1G50620	PMS1A	8	68.3
AT1G32730	PSA1	57	36.3

Figure 1. Arabidopsis SWI/SNF complex components identified in LFR-containing complexes.

(a) Gel filtration analysis of LFR-containing complexes in Arabidopsis. Immunoblotting with anti-FLAG showing the Superose 6 gel-filtration profiles of LFR-3FLAG. Top, Fraction number; Bottom, Molecular weight markers (kDa); T, Total proteins.

(b) Western blot analysis of LFR-3FLAG before and after immunoaffinity purification (IP). Total proteins were extracted from 14-day-old seedlings of Col-0 wild type (WT) or p.35S:LFR-3FLAG/lfr-1 (TR) transgenic rescued line using Anti-FLAG antibody. FT, flow through.

(c) LFR-associated proteins were detected by liquid chromatography tandem mass spectrometry (LC MS/MS). Total peptide numbers and molecular weight (MW) of each LFR-associated protein are shown.

critical for the interaction between LFR and SYD. Genetic and transcriptomic profiling analysis suggested that *LFR* and *SYD* have largely overlapped functions, especially for the development of reproductive organs. In addition, LFR and SYD interdependently bind to and activate *AG* by altering the chromatin state, including nucleosome occupancy and chromatin loop. These data suggest that LFR is a component of the SYD-containing SWI/SNF complex that promotes *AG* expression by regulating its chromatin configuration in the flower organ development of Arabidopsis.

RESULTS

Biochemical purification and identification of LFRcontaining complex

To gain an insight into the molecular function of LFR, Superose 6 gel-filtration was performed using protein extracts prepared from the p35S:LFR-3FLAG/lfr-1 transgenic complementary lines. Next, the peak of LFR-3FLAG protein was detected mainly in higher molecular complexes (near 669 kDa) by western blot, but the monomer of LFR-3FLAG (57 kDa) was totally absent (Figure 1a),

suggesting that the LFR protein may form complexes with other plant proteins. To identify interacting partners of LFR, IP-MS assays were used to isolate the LFR-containing complex respectively from a stable transgenic complementary line p35S:LFR-3FLAG/lfr-1 seedlings using LFR-3FLAG as bait (Figure 1b,c; Figure S1). Multiple SWI/SNF complex components, including SYD, SWI3D, SWP73B, ARP4, ARP7, and SYD-associated SWI/SNF complex subunit 1 (SYS1/2/3), and so on, specifically co-purified with LFR-3FLAG in three biological replicates, while no similar peptides were detected in the control extract (Figure 1c; Table S1). These data suggest that LFR is associated with SWI/SNF complexes in Arabidopsis.

LFR directly interacts with multiple SWI/SNF CRC subunits, and the N-terminal domain of SYD protein is sufficient for interaction with LFR in Arabidopsis

To confirm the interaction between LFR and SWI/SNF complexes, the yeast two-hybrid (Y2H) system was used to examine physical interactions between LFR and several subunits of the SWI/SNF complexes, such as SYD C1 (1 2009 amino acids), BRM C1 (1 921 amino acids), MINU1, MINU2, SWI3A/B/C/D, ARP4/7, SWP73A/B, and BSH. It was

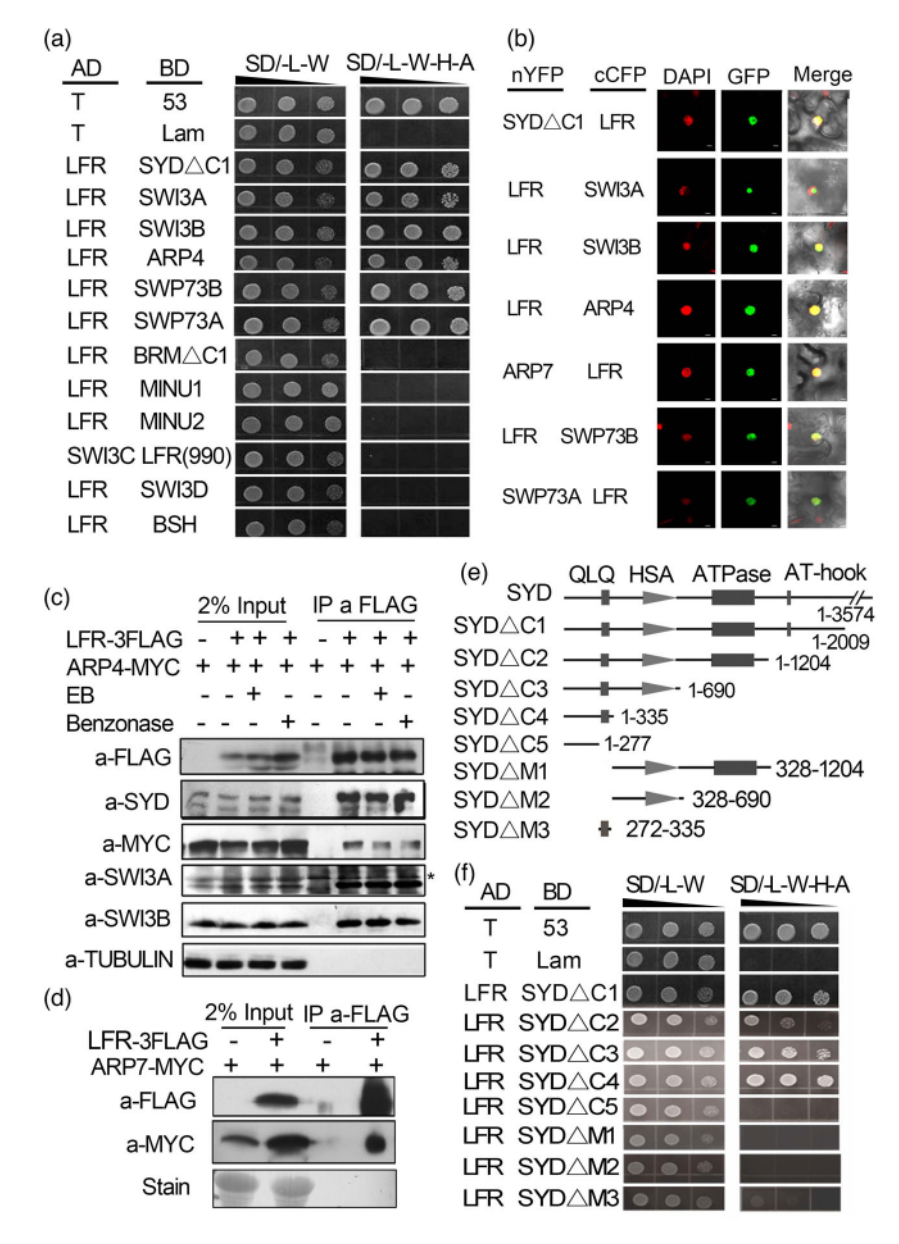


Figure 2. LFR interacts with multiple SWI/SNF subunits.

(a) LFR interacts with some SWI/SNF components in the yeast two-hybrid (Y2H) assay. The growth experiment of AH109 yeast colonies co-transformed with AD-LFR and BD-SWI/SNF genes or AD-SWI3C and BD-LFR (990, without autoactivation) on medium lacking leucine, tryptophan (SD/–L-W), and selective medium lacking leucine, tryptophan, histidine and adenine (SD/–L-W-H-A). Black triangles depict 10 fold serial dilutions (10⁻¹, 10⁻², and 10⁻³). AD-T and BD-p53 or BD-lam were used as positive or negative controls, respectively.

(b) LFR interacts with some SWI/SNF members in transiently transformed epidermal cells of *Nicotiana benthamiana* leaf in the bimolecular fluorescence complementation (BiFC) assay. 4,6-Diamidino-2-phenylindole (DAPI) signal indicates nucleus. Green fluorescent protein (GFP) signals show the protein interaction. Merge means overlay of DAPI and GFP fluorescence signals. Scale bar = 5 µm.

(c, d) LFR-3FLAG exists in the same complex as SYD, ARP4-MYC, SWI3A, SWI3B, and ARP7-MYC in the co-immunoprecipitation (co-IP) assay. Total protein extracts were derived from 14-day-old seedlings of p35S:ARP4-MYC transgenic line, or p35S:ARP4-MYC and p35S:LFR-3FLAG double transgenic line (c), and p35S:ARP7-MYC transgenic line or p35S:ARP7-MYC and p35S:LFR-3FLAG double transgenic line (d). Antibodies used for detection are labeled on the left. +/— indicates with/without corresponding protein or reagent in (c) and (d), respectively. , a non-specific band in the western blot assay for SWI3A.

(e) Schematic illustration of the SYD protein and its truncated derivatives. The SYD conserved domain, as described previously (Farrona et al., 2004) is marked on the top. Corresponding truncated protein lengths are listed below or on the right.

(f) Y2H assays for examining the interactions between different truncated versions of SYD and LFR.

found that yeast AH109 colonies co-transformed with AD-LFR, and BD-SYD C1/-SWI3A/-SWI3B/-ARP4/-SWP73A/-SWP73B grew well on the selective medium (Figure 2a),

while yeast colonies transformed with the negative controls failed to grow under the same conditions (Figure S2). Since the ARP7 elicited strong autoactivation in the yeast

AH109 strain, the Y2HGold yeast colonies co-transformed with AD-LFR and BD-ARP7 grew well on the selective medium, but not the negative control (Figure S3). These results indicate that LFR interacts directly with SYD, SWI3A, SWI3B (Lin et al., 2021), ARP4, ARP7, SWP73A, and SWP73B in yeast. However, no direct interaction was detected between LFR and BRM, MINU1, MINU2, SWI3C/D, and BSH by Y2H (Figure 2a; Figure S3).

To further confirm the interaction between LFR and these SWI/SNF subunits in plant cells, bimolecular fluorescence complementation (BiFC) assay was performed in *Nicotiana benthamiana* leaves. GFP signals were observed in nuclei co-transformed with nYFP-SYD C1/cCFP-LFR, nYFP-ARP7/cCFP-LFR, SWP73A-nYFP/LFR-cCFP, nYFP-LFR/cCFP-SWI3A, nYFP-LFR/cCFP-SWI3B, LFR-nYFP/ARP4-cCFP/, or LFR-nYFP/SWP73B-cCFP (Figure 2b); however, the series of negative controls showed no fluorescence signal (Figure S4). These results of the BiFC assay further confirmed LFR interacts with SYD, SWI3A, SWI3B, ARP4, ARP7, SWP73A, and SWP73B in plant.

Furthermore, a co-immunoprecipitation (co-IP) assay was used to determine the co-existence of LFR and SWI/ SNF complex in vivo. LFR-3FLAG and its associated proteins were immunoprecipitated from protein extracts of p35S:ARP4-MYC and p35S:LFR-3FLAG double transgenic seedlings, where the protein extracts prepared from p35S:ARP4-MYC transgenic line served as the negative control. Western blot analysis revealed the presence of ARP4-MYC, SYD, SWI3A, and SWI3B in the anti-FLAG immunoprecipitation from the double transgenic line using specific anti-MYC antibody, anti-SYD, anti-SWI3A, and anti-SWI3B (Sarnowski et al., 2002), respectively (Figure 2c). In addition, in the p35S:ARP7-MYC and p35S:LFR-3FLAG/lfr-1 double transgenic line, the presence of ARP7-MYC was detected in the immunoprecipitated complex by anti-FLAG, but not in the control lines (Figure 2d). We also carried out co-IP assay in different tissues such as seeding, inflorescence, and rosette leaves using transgenic rescued line pLFR:LFR-3FLAG/lfr-2. The results indicated that LFR is associated with the SWI/SNF components, SWI3A and SWI3B, in different tissues (Figure S5). To exclude the possibility that LFR interacts with these proteins dependent on the existence of DNA, nucleic acid enzymes (benzonase) or ethidium bromide (EB), capable of digesting DNA or preventing DNA-protein complex formation, respectively, were added, and the results showed that they did not affect the co-precipitation of LFR and SWI/SNF complex (Figure 2c). Taken together, these results indicate that the interactions between LFR and SWI/SNF complex, such as SYD, SWI3A, SWI3B, ARP4, and ARP7 were stable and independent of DNA in Arabidopsis.

Given that SYD is the only SWI/SNF core ATPase that directly interacted with LFR in the Y2H experiment, the domains of SYD that were responsible for its interaction

with LFR were mapped. It was found that SYD C5, SYD M1, and SYD M2, which lack N-terminal region containing the QLQ domain, did not interact with LFR. However, SYD M3, which only contains the QLQ domain, did not interact with LFR either (Figure 2e,f). These results showed that the N-terminal region of SYD including the QLQ domain (SYDC 4) is required for LFR interaction.

LFR genetically interacts with SYD during filament and pistil development

To unravel the genetic relationship between LFR and the SWI/SNF core ATPase SYD, a null mutant of syd-5 in the Col-0 ecotype (Bezhani et al., 2007) was crossed with the null mutant of Ifr-2 to get the Ifr-2 syd-5 double mutant (dm). The single and double mutants were identified at the RNA and protein levels (Figure 3a c). These experiments revealed the lack of transcriptional- or protein-level regulation between LFR and SYD (Figure 3a c). Interestingly, Ifr-2 and syd-5 mutants had similar defects in stamens and pistils, such as shorter stamen filaments (Figure 3d,f), abnormal pistils with decreased carpel number, and elongated internodes (Figure 3e,g). Furthermore, the Ifr-2 syd-5 double mutant showed similar defects of pistils and stamens to the single mutants with no phenotype enhancement (Figure 3d g). These results indicate that LFR and SYD are essential for male and female reproductive organ development, supporting the notion that LFR and SYD act in the same complex in the floral organ development regulation.

LFR and SYD co-regulate transcription of a subset of genes

To further reveal the overlapping molecular roles of LFR and SYD, transcriptome profiling data was generated for wild-type, Ifr-2, and syd-5 inflorescences using ATH1 microarrays. A total of 1271 differentially expressed genes (DEGs) genes (Fischer's exact P-value >0, |FC| > 2) were identified in Ifr-2 or syd-5 relative to the wild type (Figure 4a; Figure S6; Table S2). Of these, 1089 genes displayed a significantly altered expression in Ifr-2 relative to the wild type (q-value <5 , |FC| > 2), including 354 up- and 735 down-regulated genes; and a total of 528 genes displayed a significantly altered expression in syd-5, including 285 up- and 243 down-regulated genes (Figure 4b; Table S2). To address whether LFR and SYD have similar targets or regulate similar processes, the genes differentially expressed in Ifr-2 were compared to those differentially expressed in syd-5. Interestingly, there was a significant overlap for genes repressed (155 genes) or activated (134 genes) by both LFR and SYD (Figure 4b; Table S2). Gene ontology (GO) term enrichment analysis of genes whose expression was affected in both mutants revealed enrichment of genes linked to stimuli response (stress, external, and endogenous cues), which is consistent with SYD preferentially targeting stimulus-responsive

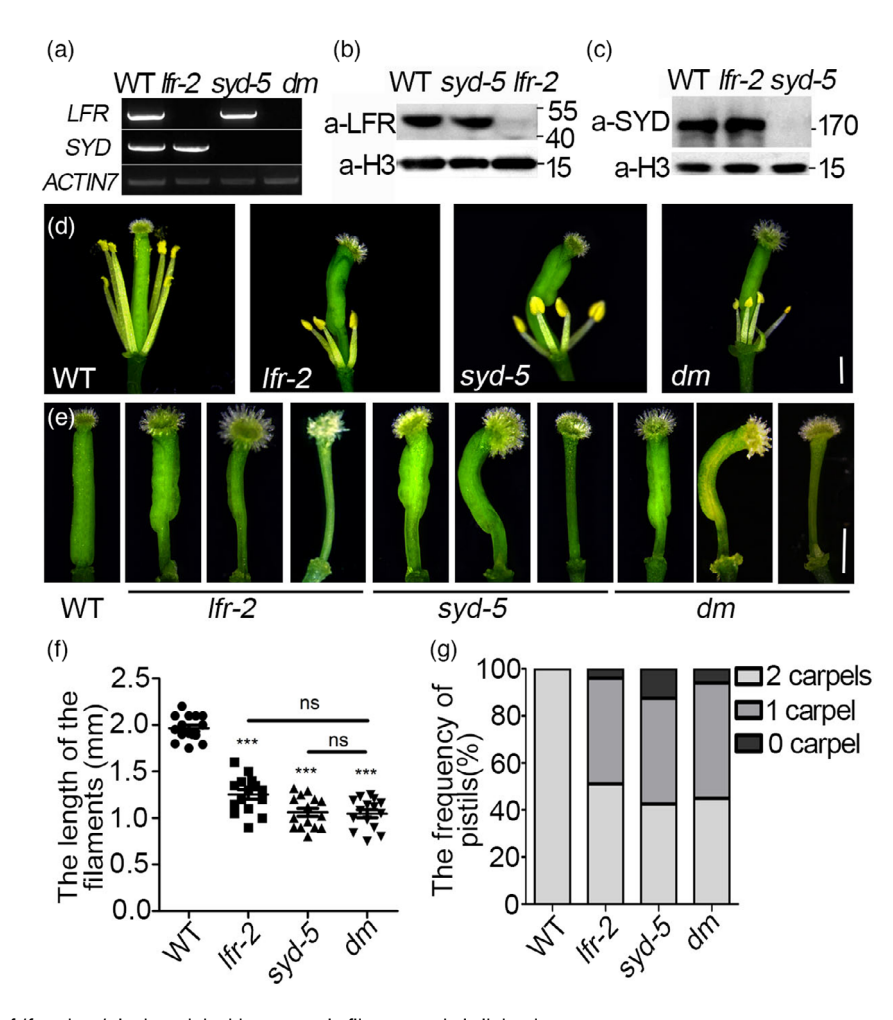


Figure 3. Phenotypes of *Ifr* and *syd* single and double mutants in filament and pistil development.
(a) Transcript levels of *LFR* or *SYD* were detected by RT-PCR in wild type, *Ifr-2*, *syd-5* single and double mutants (*dm*). The template RNA was isolated from 14-day-old seedlings of the indicated genotypes. Transcript levels were normalized to *ACTIN7*.

genes and hormone pathways (Bezhani et al., 2007; Shu et al., 2021); as well as the regulation of gene expression, transport, organ growth, and development (Figure 4c; Table S2). A total of 16 genes were selected for Reverse Transcription-Quantitative Real-Time Polymerase Chain Reaction (RT-qPCR) validation of differential expression in both *lfr-2*, *syd-5*, and *dm* mutants, including 8 down- and 8 up-regulated genes. In all tests, the RT-qPCR data supported the microarray data (Figure 4d); thus, the results suggested that LFR and SYD may co-regulate a subset of gene expression.

Taken both the physical interaction between LFR and SYD together, similar floral defects of the single and double mutants, as well as largely overlapping transcriptome

data strongly suggest that LFR acts in a manner similar to SYD for regulating a subset of gene expression in plants.

Filament and pistil defects in *Ifr 2, syd 5,* and *Ifr 2 syd 5* double mutants are partially attributable to the downregulation of *AG* expression

To elucidate the molecular role of *LFR* and *SYD* in floral organ development, microarray data were explored and revealed that several MADS-box ABCE genes involved in floral organ identity were misregulated in *Ifr-2* and *syd-5* mutants (Figure 5a). The expression level of these genes was further confirmed by RT-qPCR in *Ifr-2*, *syd-5*, and double mutants. In *Ifr-2* mutants, it was found that class A (*AP1*), B (*AP3* and *P1*), and C (*AG*) floral homeotic gene

⁽b, c) Western blot assays were performed to analyze the protein level of LFR and SYD in nuclear protein extracted from 14-day-old seedlings in genotypes as indicated using anti-LFR antiserum (b), and anti-SYD (c), respectively. Histone H3 was used as loading control.

indicated using anti-LFR antiserum (b), and anti-SYD (c), respectively. Histone H3 was used as loading control. (d, e) Arabidopsis flowers at stage 13 after removing the sepals and petals to show the stamen (d) and pistils (e) in WT, Ifr-2, syd-5, and dm. Scale bar = 1 mm.

⁽f) Statistical analysis of filament length in stage 13 flowers in WT, Ifr-2, syd-5, and dm. Significant statistical differences were tested via Student's t-test (P < 0.001), n 15, ns, not significant.

⁽g) Percentage of pistils with different carpel number in stage 13 flowers in WT, Ifr-2, syd-5, and dm. n 30.

Figure 4. Genes misexpressed in Ifr-2 and syd-5 inflorescences.

(a) Heat map showing the differentially expressed genes in three replicates of microarray data of *lfr-2* or *syd-5* mutants. Red and blue represent up- and down-regulation in mutants, respectively (1271 misregulated genes in total).

1365313x, 2023, 2. Downloaded from https://onlinelibrary.wiley.com/doi/10.1111/pj.16385 by University Of Pennsylvania, Wiley Online Library on [1905/2024]. See the Terms and Conditions (https://onlinelibrary.wiley.com/terms-and-conditions) on Wiley Online Library for rules of use; OA articles are governed by the applicable Creative Commons License

⁽b) Venn diagrams showing statistically significant overlaps between genes up- or down-regulated in Ifr-2 and syd-5. P > 0, hypergeometric test.

⁽c) Gene ontology (GO) enrichment analysis of DEGs in Ifr-2 and syd-5 mutants.

⁽d) RT-qPCR validation of gene expression changes in the microarray assay. Bars indicate the mean \pm SD of three independent biological repeats. *EAF4a1* was used as an internal control. The *y*-axis was set in two segments to show both the upregulated and downregulated genes in the same graph.

1365313x, 2023, 2, Downloaded from https://onlinelibrary.wiley.com/doi/10.1111/tpj.16385 by University Of Pennsylvania, Wiley Online Library on [19/05/2024]. See the Terms and Conditions (https://onlinelibrary.wiley.com/rems-and-conditions) on Wiley Online Library for rules of use; OA articles are governed by the applicable Creative Commons License

expression was dramatically reduced relative to the wild type (Figure 5b). In syd-5 mutants, the expression level of AP1 and AG was dramatically reduced relative to the wild type; and the class B gene expression showed a slight, albeit insignificant reduction in our growth conditions (Figure 5b). These gene expression levels in double mutants were almost similar to those of the single mutant (Figure 5b). In agreement with previous reports, SYD is a positive upstream regulator of AG (Wu et al., 2012), and it was found that the AG expression was dramatically reduced in syd-5 single and double mutants (Figure 5b). To further confirm the down-regulation of the AG gene, the construct of β-alucuronidase (GUS) driven by the AG promoter and the second intron (pAGi:GUS) (Sieburth & Meyerowitz, 1997) was introduced into Ifr-2 and syd-5 single or double mutants. In agreement with previous reports, the GUS reporter was expressed in developing whorls 3 and 4 of the flowers, especially in pistils and filaments. The GUS reporter signals were reduced in the pistils and filaments of Ifr-2 and syd-5 single mutants (Figure 5c). Similar GUS signal reduction was observed in Ifr-2 and syd-5 double mutants comparable to that in single mutants (Figure 5c). To further confirm the histological staining result, GUS fluorometric assay was used to quantify the GUS activity of the pAGi:GUS in different genotypes. In agreement with GUS staining and RT-gPCR results, the GUS activity of the pAGi:GUS was reduced in single and double mutants compared with the wild type (Figure 5d). AG was reported to control filament elongation and pistil development (Ito et al., 2007); thus, these results possibly indicate that the down-regulation of AG expression may partially account for the filament and pistil defects in Ifr-2 and syd-5 mutants.

To further test whether the filament and carpel defects in Ifr-2 and syd-5 result from the down-expression of AG, we introduced the construct of p35S:AG (Wu et al., 2012) into Ifr-2 and syd-5 single mutants. We observed the filament and carpel phenotypes of three independent lines showing an obvious overexpression of AG in the inflorescence of Ifr-2 and syd-5 mutants background (Figure 5e g; Figure S7). The reduced length of filament and carpel number defects of Ifr-2 and syd-5 single mutants flowers were partially rescued by p35S:AG (Figure 5e i; Figure S7). This is consistent with previous research that AG controls filament elongation and carpel development (Ito et al., 2007). Thus, these results indicated that the downregulation of AG expression partially accounts for filament and carpel defects in Ifr-2 and syd-5 mutants.

LFR and SYD interdependently bind to AG chromatin

Previous studies suggested that SYD binds to specific sites in the second intron of AG to activate its expression during flower development (Wu et al., 2012). Since LFR shows not only physical and genetic interaction with SYD but also a similar positive role on AG expression to that of SYD, we hypothesized that LFR may also directly regulate AG expression. Therefore, the association of LFR with AG chromatin by ChIP was assessed with the stable transgenic complementary line pLFR:LFR-3FLAG/lfr-2 inflorescence (Figure 6). A total of 10 fragments were selected and distributed in the promoter, as well as 5-UTR (p1-p7), intron (AGi1-i2), and 3-UTR (down) of AG (Figure 6a). The ChIP-gPCR data showed that the promoters p3 and p4, and second intron AGi2 fragments were reproducibly amplified from chromatin of pLFR:LFR-3FLAG/lfr-2 immunoprecipitated with anti-FLAG; however, no such enrichment was detected in the negative control of the wild type (Figure 6b). In addition, it was found that SYD showed a similar binding pattern as LFR, including the promoters p3 and p4 (Figure 6c), and the previously reported region of AGi2 in pSYD:GFP-SYD C1/syd-5 transgenic complemented line (Wu et al., 2012), in which SYD C1 was used because it was shown to be sufficient for its biological activity (Su et al., 2006). These results provided evidence of LFR directly binding to AG chromatin in a similar pattern to SYD.

To address the interdependency of LFR and SYD in the association with the target gene, a ChIP-gPCR assay with anti-SYD and anti-LFR antiserum was performed in wild type, Ifr-2, and syd-5 inflorescence. In the absence of functional LFR or SYD, their enrichment to AG was nearly reduced to background level similar to the negative control

Figure 5. LFR and SYD regulate transcription of several MADS-box ABCE genes.

⁽a) Heatmap of selected MADS-box ABCE genes in three independent biological repeats of microarray data for Ifr-2 and syd-5 mutants. Fold-change in gene expression was log2-transformed and represented as: red, upregulated; blue, downregulated.

⁽b) RT-qPCR data for the transcript level of five major floral homeotic MADS genes in different backgrounds as indicated. The total RNA was isolated from the inflorescence of WT or various mutants. Transcript levels were normalized to the loading control gene eAF4A1.

⁽c) GUS staining assay of the inflorescence (upper), and the flowers at stage 13 (bottom) of pAGi:GUS in WT, Ifr-2, syd-5, and double mutant background.

⁽d) Quantitative fluorometric GUS assays of the inflorescence of pAGi:GUS in WT, Ifr-2, syd-5, and double mutant background.

⁽e, f) Arabidopsis flowers at stage 13 after removing the sepals and petals to show the stamen (e) and pistils (f) in p35S:AG 1 2 in WT, Ifr-2 and syd-5 mutant background.

⁽g) RT-qPCR data for the transcript level of AG in multiple p35S:AG 1 2 transgenic lines in different background. Transcript levels were normalized to loading control gene eAF4A1.

⁽h) The statistical data of filament length from stage 13 flowers in multiple p.35S:AG 1.2 transgenic lines in different mutant background, n > 20.

⁽i) The percentage of carpel number from stage 13 flowers in multiple p35S:AG 1 2 transgenic lines in different background, n > 20. Significant statistical differences were tested using Student's t-test (P < 0.05; P < 0.01; P < 0.001; ns, not significant). Scale bar = 0.5 cm (c) and 0.2 mm (e, f).

(Figure 6d,e). Since it was shown that the protein level of LFR in *syd-5* was almost comparable to that in the wild-type control and vice versa (Figure 3b,c), this eliminated the possibility that binding reduction may result from low LFR or SYD levels in *syd-5* or *lfr-2* mutants, respectively.

Collectively, these results demonstrated that LFR and SYD are interdependently associated with *AG* chromatin.

1363313x, 2023, 2, Downbaded from https://onlinelibrary.wiley.com/doi/10.1111/tpj.16385 by University Of Pennsylvania, Wiley Online Library on [1905/2024]. See the Terms and Conditions (https://onlinelibrary.wiley.com/terms-and-conditions) on Wiley Online Library for rules of use; OA articles are governed by the applicable Creative Commons License

To investigate whether other ABCE-class genes are direct targets of LFR and SYD, we performed ChIP-qPCR assay in pLFR:LFR-3FLAG/lfr-2 or pSYD:GFP-SYD C1/syd-5

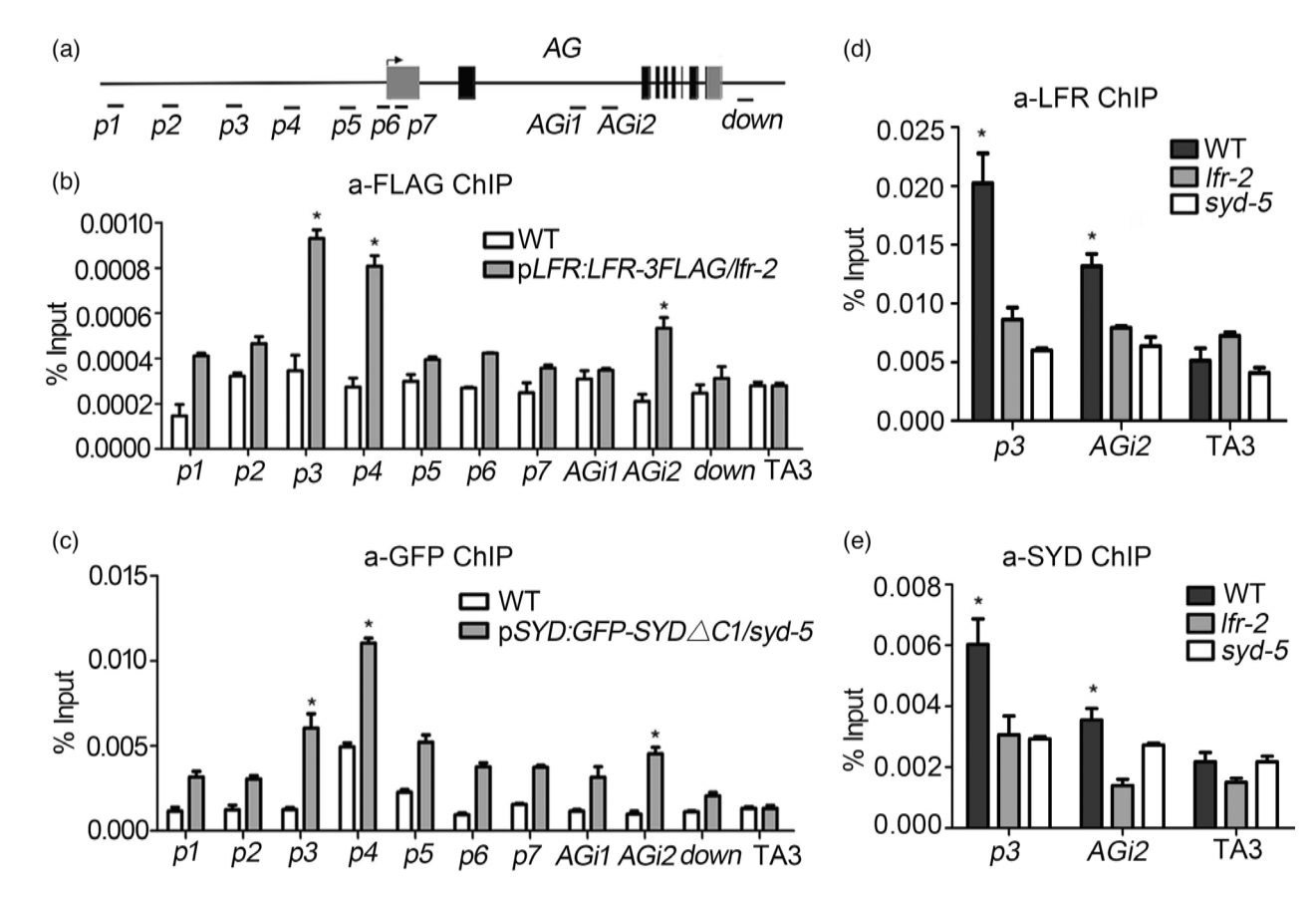


Figure 6. LFR and SYD interdependently bind to AG chromatin in flower development.

(a) Diagrams of AG gene structures: Black boxes indicate exons, gray boxes are untranslated regions, and long black lines represent the promoter, introns, and 3 terminal sequences, respectively. The black arrow represents the transcription start site (TSS), and the black lines below the gene structures represent PCR fragments tested in chromatin immunoprecipitation (ChIP)-quantitative (q) PCR in (b e) and Figure 7a,b.

(b, c) LFR and SYD bind to the AG chromatin in ChIP-qPCR assay using anti-FLAG antibody (a-FLAG) (B), and anti-GFP antibody (a-GFP) (C) in inflorescence of transgenic complementary lines as indicated.

(d, e) Association of LFR and SYD with the AG chromatin in ChIP-qPCR assay using the polyclonal anti-LFR antiserum (a-LFR) (d) or anti-SYD (a-SYD) (e) in WT, syd-5, and Ifr-2 inflorescence. For (b e), three biological replicates were carried out, and similar results were obtained. Bars represent the means \pm SD of the three technological replicates from one representative biological replicate. Significant statistical differences were tested via Student's t-test (P < 0.05). A retrotransposon locus TA3 (At1g37110) was used as the negative control.

inflorescences. The ChIP-qPCR data showed that LFR and SYD are associated with the promoters and TSS region of AP1, AP3, and PI (Figure S8a). We found that LFR, but not SYD, can bind to SEP3 (Figure S8b). These results indicated that LFR and SYD may have largely overlapping functions in regulating the ABC genes in floral organ

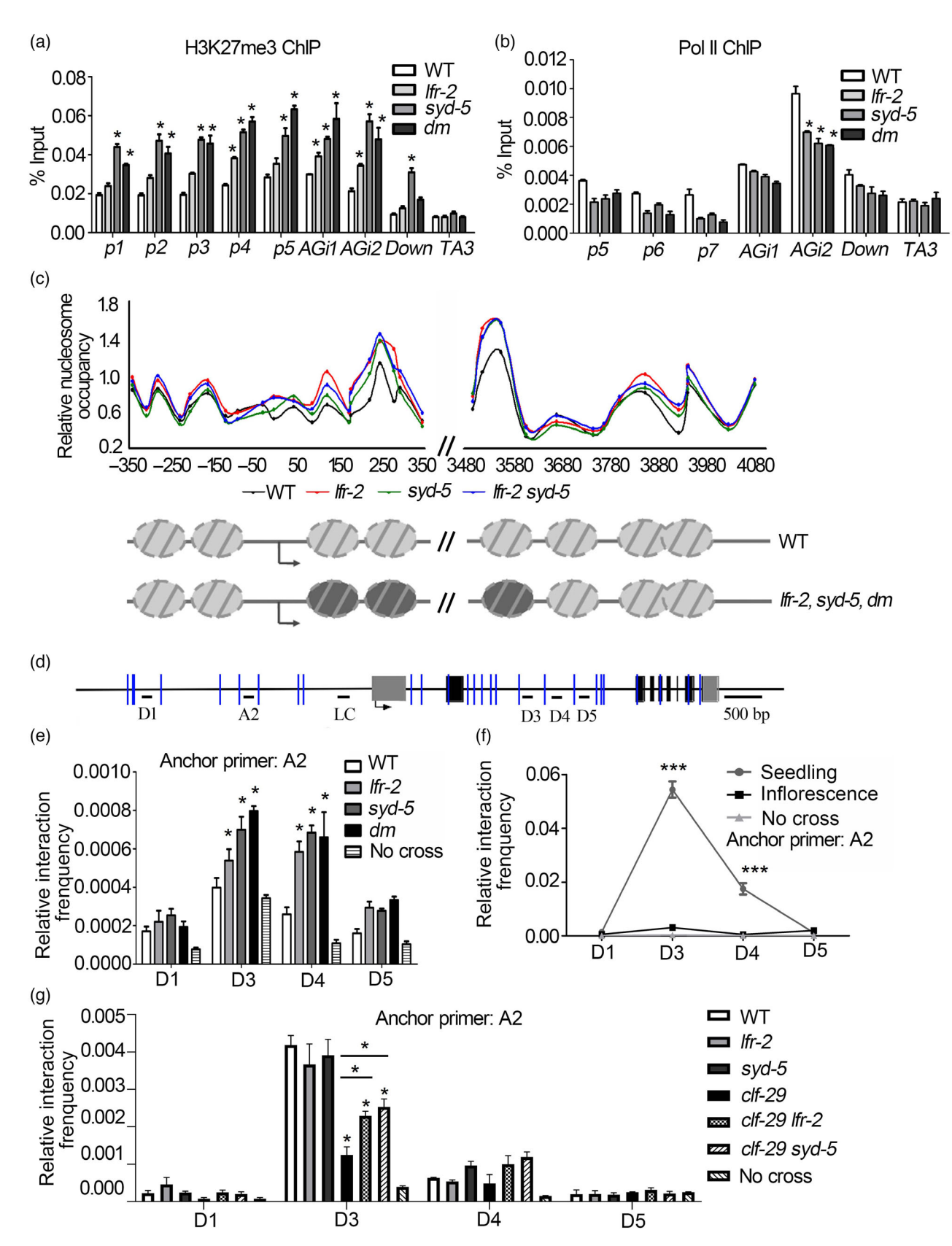
Figure 7. LFR and SYD affect AG gene chromatin configuration.

(a, b) ChIP-qPCR analysis of H3K27me3 modification (a), and Pol II enrichment levels (b) on AG chromatin in Col-0, Ifr-2, syd-5, and double mutant inflorescence. A retrotransposon locus TA3 (At1g37110) was used as the negative control.

(c) Relative nucleosome occupancy in a region including the TSS region (-350 350 bp), and the second intron including the i2 fragment (3480 4080 bp) of AG in inflorescence. Upper panel: nucleosome occupancy detected by MNase-qPCR in WT (black), Ifr-2 (red), syd-5 (green), and double mutants (dm, blue). The -73 position of gypsy-like retrotransposon (At4g07700) was used for the control. X-axis values denote the distance (bp) from TSS. Lower panel: schematic diagram of position and occupancy of the nucleosome in WT, Ifr-2, syd-5, and double mutants. Gray ovals with two gray lines represent positioned nucleosomes in WT, and the relative increase of nucleosome occupancy in the mutants is shown by black ovals. Three biological replicates were performed, and similar results were obtained. Values depict the mean of three technical replicates from one representative experiment.

(d) Diagrams of AG gene structures, where blue vertical lines represent the NIallI and DpnII restriction sites. The black arrow depicts TSS, while the black short horizontal lines below the gene model represent the positions of primers used in the chromosome conformation capture (3C)-qPCR assay in (e, f). LC was used as the loading control.

(e g) 3C-qPCR assay to detect chromatin loop of the AG locus using A2 as the anchor region in WT, Ifr-2, syd-5, and dm inflorescence (e), 14-d-old wild-type inflorescence and seedlings (f), and wild-type, Ifr-2, syd-5, clf-29 single and several double mutant seedings (g). Relative interaction frequencies were calculated as described in Methods. At least two biological replicates were conducted, and similar results were obtained. Values represent means of the three technology replicates from one representative experiment, while error bars depict SD. Significant statistical differences were tested by Student's t-test (P < 0.05, P < 0.001).



1365313x, 2023, 2, Downbaded from https://onlinelibrary.wiley.com/doi/10.1111/tpj.16385 by University Of Pennsylvania, Wiley Online Library on [1905/2024]. See the Terms and Conditions (https://onlinelibrary.wiley.com/terms-and-conditions) on Wiley Online Library for rules of use; OA articles are governed by the applicable Creative Commons License

development. However, they may also have some different/specific targets because LFR is also involved in the MINU-containing chromatin remodeling complex.

LFR and SYD regulate AG expression by influencing histone modification and Pol II enrichment levels

The modification level of the trimethylation of histone H3 Lys27 (H3K27me3) accounts for an important negative effect on AG expression (Lee et al., 2022; Wellmer et al., 2006; Wu et al., 2003, 2012; Xiao, Jin, Yu, et al., 2017). Here, the H3K27me3 level of AG was examined by ChIPqPCR experimental analysis in the wild type, syd-5, Ifr-2, and Ifr-2 svd-5 double mutants. The H3K27me3 levels markedly increased in Ifr-2, syd-5, and Ifr-2 syd-5 inflorescence (Figure 7a). In addition, the recruitment of RNA polymerase (Pol II) was also examined, revealing that it was reduced in syd-5, Ifr-2, and Ifr-2 syd-5 mutants compared with that in the wild type at the AG regulatory regions (Figure 7b). Taken together, the increase of H3K27me3 level and reduced recruitment of Pol II at the AG locus are in accordance with the downregulated expression of AG in syd-5, Ifr-2, and Ifr-2 syd-5 mutants (Figure 5a,b).

LFR and SYD participate in nucleosome occupancy and gene loop at AG locus

Since the SWI/SNF chromatin remodelers affect the accessibility of the genomic DNA by altering the occupancy or positioning of nucleosomes (Clapier & Cairns, 2009; Sacharowski et al., 2015), the effect of LFR or SYD mutation on the accessibility of the AG locus was then monitored here. Nucleosome positioning and occupancy around the transcription start site (TSS), and the second intron region (including AGi2 fragment of AG in wild-type and mutant inflorescence) were examined via micrococcal nuclease (MNase)-gPCR. The DNA fragments protected by nucleosomes from MNase digestion were mapped near the TSS region and second intron at the AG locus in the wild type (Figure 7c). Notably, the increase of nucleosome occupancy in the region exactly downstream of TSS (nucleosomes localized between ~75 to ~350 bp), and near the LFR- and SYD-binding site in intron 2 at the AG locus (AGi2; localized between ~3480 to ~3580 bp) in syd-5, Ifr-2, and Ifr-2 syd-5 mutants were consistently reproduced, compared with that of the wild type (Figure 7c). No strong change in nucleosome occupancy or positioning was observed at the control locus, a gypsy-like retrotransposon gene (At4g07700) in wild type and mutants (Figure S9). These results demonstrated that LFR and SYD may be required to reduce nucleosome occupancy at some specific AG loci.

As stated, the present ChIP-qPCR data showed that LFR and SYD simultaneously bind to the promoter and second intron (~3-kb long) of AG, and are required for its transcriptional activation. Since the chromatin loop is reported to play a role in transcriptional regulation (Cavalli & Misteli, 2013; Jegu et al., 2014), quantitative chromosome conformation capture (3C) experiments were also performed using wild-type and mutant inflorescences to test for a high-order chromatin structure in AG, as well as the possible regulatory role of SYD and LFR during chromatin structure formation. We selected multiple segments in the promoter (D1 and A2), and second intron regions (D3, D4, and D5) of the AG gene (Figure 7d). Significant increases in gene loop formation of the AG gene were detected in Ifr-2 and syd-5 single and double mutant inflorescences compared to that in the wild type and non-crosslinked control (Figure 7e: Figure \$10). These results indicate that the chromatin loop at the AG locus may restrict its transcription, and LFR-SYD may play a negative role in the establishment and/or stability of chromatin loop at the AG locus.

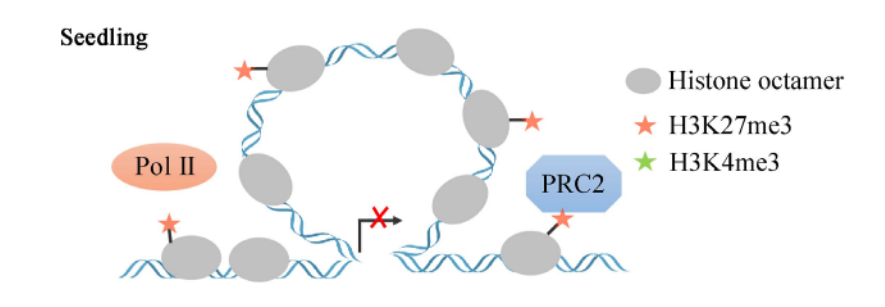
Gene loop at AG locus is required for gene silence in seedling

Since the AG gene is differentially expressed in the vegetative (silent) and reproductive stages (active), the relationship between the silent or active state of AG with the gene loop formation in seedling or inflorescence was further analyzed. Notably, it was found that there was a chromatin loop between the promoter and second intron of AG in the wild-type seedlings, but not in the inflorescences or the non-crosslinked control (Figure 7f; Figure S11); thus, the results indicated that the gene loop at AG locus may also contribute to gene silencing in seedlings.

To further confirm the possible biological significance of the chromatin loop in AG expression level and the roles of LFR, SYD, and CLF in seedling chromatin loop formation, we first tested the chromatin loop in clf-29 seedling. The 3C assay and RT-qPCR data showed that a dramatic loss of chromatin loop was detected in clf-29 in seedlings, which showed ectopic expression of AG in seedlings (Figures 7g; Figures S12 and S13). We found that the removal of LFR or SYD in the clf-29 background partially represses the chromatin loop loss and ectopic expression of the AG gene in clf-29 (Figure 7g; Figure S12), which is consistent with the ChIP data showing that LFR and SYD can bind to AG chromatin in clf-29 mutant, but not in wildtype seedlings (Figure \$14). These results indicated that the chromatin loop formation is negatively correlated with the expression level of AG and CLF may promote the chromatin loop formation to repress its expression by antagonizing with LFR and SYD.

Taken together, these results suggest that LFR and SYD target the AG gene, reduce the nucleosome occupancy, inhibit the chromatin loop formation and H3K27me3 modification, and maintain high Pol II levels to guarantee an active state of AG expression during floral organ development. Regarding the vegetative growth,

490 Xiaowei Lin et al.



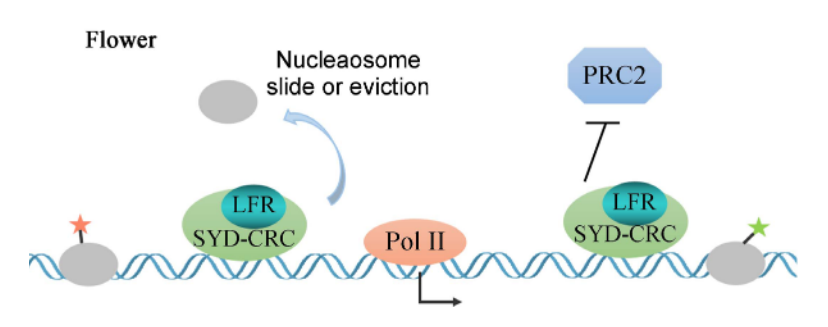


Figure 8. Modeled role of LFR-SYD-chromatin remodeling complex (CRC) in the control of AG gene transcription. During vegetative growth, the PRC2 complex, including CLF, inhibits LFR and SYD from targeting the AG gene (Present study; Wu et al., 2012). The AG gene formed a chromatin loop, inhibiting AG transcription. In reproductive growth, LFR-SYD CRC was recruited to the AG locus and maintained relatively low nucleosome occupancy, chromatin loop, and H3K27me3 modification levels, as well as a high Pol II level to guarantee an active state of AG expression in floral organ development.

however, a chromatin loop is formed at the AG chromatin to repress its transcription (Figure 8).

DISCUSSION

LFR functions as a SYD-containing SWI/SNF CRC component

Plant SWI/SNF complexes are pivotal for the appropriate gene expression across a wide range of processes in response to environmental and developmental cues, and numerous recent studies have provided important insight into the subunit composition and mode of action of plant BRM-containing SWI/SNF complexes (Jaronczyk et al., 2021; Yu et al., 2020, 2021). SYD may be a plant-specific SWI/SNF ATPase that is distinct from BRM, as well as its yeast and mammal orthologs, in that it lacks the Bromodomain for acetylated-histone tail binding in the Cterminus (Wagner & Meyerowitz, 2002); however, the plant-specific SYD-containing complex remains to be fully elucidated. LFR is an ARM-repeat domain-containing protein, which has been predicted to be a subunit of the SWI/SNF complex (Wang et al., 2009). Yet, the compelling biochemical, molecular, and genetic evidence is largely missing. In the present study, detailed analyses showed that LFR is stably associated with the SWI/SNF complex in Arabidopsis using IP-MS, BiFC, Y2H, and co-IP approaches (Figures 1 and 2). Among the four SWI/

SNF complex core ATPases, it was found that SYD stably interacts with LFR across all different methods used in this study (Figure 2a,b). It was also demonstrated that LFR is stably co-immunoprecipitated with SYD independent of DNA (Figure 2c). Interacting domain analysis revealed that the N-terminal domain, including QLQ of SYD, is important for interaction with LFR (Figure 2e); thus, supporting evidence has been provided that LFR may be a SYD-containing SWI/SNF component. Our data is also consistent with LFR being a component of a MINU1/2 ATPase-containing SWI/SNF complex (Diego-Martin et al., 2022), although in this case, the interaction between LFR and MINU1/2 would be indirect. During the review of our manuscript, two recent studies reported that LFR is involved in both the SAS and MAS complex (SYD- and MINU1/2-associated SWI/SNF complexes) (Fu et al., 2023; Guo et al., 2022), which serves as supports of our work. Indeed, multiple SAS or MAS components were specifically co-purified with LFR-3FLAG in our IP-MS assays (Figure 1c). For example, ARP4 and ARP7, SWIP73B, BDH1/2 (BCL7A/B), and ACTIN2/7 are SAS- and MAS-shared components; SYD, SWI3D, and SYS1/2/3 (SSIP1/2/3), are SAS-specific components; MINU1/2, SWI3A, SWI3B, BSH, TPF1/2 (PMS1A), BRD5, and PSA1 (MIS) are MAS-specific components. LFR is a noncatalytic subunit with three ARM-repeat domains homologous to human ARID1/2 (Hernandez-Garcia et al., 2022).

1365313x, 2023, 2. Downloaded from https://onlinetibrary.wiley.com/doi/10.1111/pj.16385 by University Of Pennsylvania, Wiley Online Library on [19/05/2024] See the Terms and Conditions (https://onlinelibrary.wiley.com/terms-and-conditions) on Wiley Online Library for rules of use; OA articles are governed by the applicable Creative Commons License

The ARM domains of ARID1 interact with the core ATPase and all other Base subunits and play pivotal roles in the complex organization (He et al., 2020; Mashtalir et al., 2020). In addition, the ARID1 subunit is required for nucleosome sliding activity (He et al., 2020). Though LFR lacks the ARID domain for DNA binding compared with ARID1/2 (Hernandez-Garcia et al., 2022), this structural and biochemical information helps us to unravel the detailed contribution of LFR to the SWI/SNF complexes in the future.

LFR directly activates AG expression by altering chromatin structure together with SYD in stamen and pistil development

Recent reports have not only identified the new subunits of BRM-SWI/SNF complexes but also examined the genetic relationship between brm-1 and brip1/2 or brd1/2/13, for which the multiple mutants did not exacerbate the defects of the null mutant brm-1, thereby showing that they act in the same complex (Jaronczyk et al., 2021; Yu et al., 2020, 2021). In contrast to brm, the genetic relationship between syd and its possible complex partner remains unknown. The loss of Ifr, as it was named a Leaf and Flower Related gene, resulted in defects in the leaf and flower. Though the possible molecular mechanism in leaf development is unraveled (Lin et al., 2018, 2021), the mechanisms of floral organ defects remain elusive. The present results demonstrated that LFR and SYD not only interact with each other but also show similar floral organ defects, while Ifr did not enhance the syd-5 phenotype, indicating that they function within the same complex (Figure 3). Transcriptome data also showed that LFR and SYD may co-regulate a subset of gene expression, including the well-established ABC model genes in floral organ identity specification (e.g., AG; Figures 4 and 5). LFR and SYD interdependently co-targeted to AG chromatin, reduced nucleosome occupancy, altered the chromatin configuration, decreased the H3K27me3 modification level, and increased the Pol II association for the success of AG transcription (Figures 6 and 7), ensuring normal male and female reproductive organ morphology (Figure 8). In addition, Ifr-2 and syd-5 mutants both produced small rosettes, were dwarfed with reduced apical dominance, and exhibited sterile defects (Figure S15; Wagner & Meyerowitz, 2002; Wang et al., 2009), for which the underlying molecular mechanisms are of great importance, but remain to be revealed. Future studies are thus required to identify more common target genes directly regulated by LFR and SYD-containing /SNF complexes in Arabidopsis.

AG is subjected to higher chromatin conformation regulation by CLF and SWI/SNF complexes

In Arabidopsis, the only C-class gene AG encodes a MADSbox transcription factor that exerts critical roles in

reproductive organ development (Bowman et al., 1991; Dennis & Peacock, 2019; Ito et al., 2004; Krizek & Fletcher, 2005; Liu et al., 2014; Yanofsky et al., 1990). The AG gene is silenced in seedlings but is activated in early floral primordia during the reproductive phase. Different epigenetic mechanisms are involved in the spatiotemporal expressions of AG. A \sim 3 kb second intron of AG is critical for its expression, in that it produces several intronic ncRNAs (incRNAs) to repress AG transcription (Pelayo et al., 2021). The present results further showed that the LFR and SYD-containing SWI/SNF chromatin remodeling complex activate AG expression by binding to both the promoter and second intron and inhibit chromatin loop formation at the AG locus in floral organ development (Figure 7f,g). In the wild-type seedlings, CLF may promote the repressive chromatin loop formation to silence AG (Figure 7g; Figure S12), which is consistent with the previous research that Polycomb group proteins (PcGs) mediate repressive chromatin loops formation to facilitate the gene silencing in Drosophila and Arabidopsis (Kim et al., 2021; Ogiyama et al., 2018; Sun et al., 2023). Since LFR and SYD can successfully bind to AG chromatin in clf-29 mutant, but not in wild-type seedlings (Figure S14), and the removal of LFR or SYD in the clf-29 background partially repressed the chromatin loop loss and high expression of AG gene in clf-29 (Figure 7g; Figures S12 and S13), indicating that LFR and SYD may also inhibit chromatin loop formation at the AG locus in clf-29 seedlings. Together, these results demonstrated that CLF may promote repressive chromatin loop formation and repress this floral identity gene by inhibiting the association of LFR and SYD to the AG locus to ensure flattened leaf formation in vegetative growth. However, we notice that the removal of LFR/SYD only partially rescued the chromatin loop down-regulation in clf-29, but not to the wild-type level. The possible reasons are as follows: i, the mutation of CLF led to the failure of some of the loop formation; ii, besides LFR and SYD, there could be some other epigenetic factors that are required to block the chromatin loop formation. Since SYD was reported to act as trithorax proteins to reverse the PcG repression (Wu et al., 2012), ATX1, a member of the trithorax complex counteracting repression by Polycomb group (PcG) complexes (Alvarez-Venegas et al., 2003; Carles & Fletcher, 2009), and its paralogs may also inhibit the chromatin loop similar to LFR/SYD.

The abovementioned results allow us to elucidate the effect of the chromatin loop in AG transcriptional regulation. It was also demonstrated that the SWP73B/BAF60 subunit of the SWI/SNF complex plays a negative role in the gene loop formation to reduce the expression of FLC, and induce flowering after vernalization (Jegu et al., 2014). These results show that LFR-SYD and BAF60 may play similar negative roles in the gene loop formation, and/or stability of the chromatin loop, at least at AG or FLC loci,

492 Xiaowei Lin et al.

respectively. Consistently, a high-throughput genome-wide analysis, combining Hi-C, histone modification, nucleosome positioning, and density, as well as gene expression in *brm* showed that the SWI/SNF chromatin remodeling complexes regulate genome architecture in Arabidopsis (Yang et al., 2022).

In summary, deeper insight into the composition and mode of action of the Arabidopsis SYD-SWI/SNF complex has been provided by unraveling the biochemical, molecular, and genetic relationship between LFR and SYD, which independently bind to, and directly open the chromatin configuration for active AG transcription. These results allow for the molecular mechanism of the SYD-SWI/SNF complex to be deciphered, which is essential for higher chromatin conformation of floral identity genes in reproductive organ development.

MATERIALS AND METHODS

Plant materials and growth conditions

All plants used in this study were in the Col-0 ecotype. The *Ifr-2* mutant and p35S:LFR-3FLAG/Ifr-1 transgenic line were described previously (Lin et al., 2021; Wang et al., 2009). The *syd-5* (SALK_023209) obtained from Arabidopsis Biological Resource Center (ABRC) was reported by Bezhani et al. (2007) and Shu et al. (2021). The pLFR:LFR-3FLAG/Ifr-2 was generated by our previous work (Ma et al., 2023). p35S:ARP4/Col, p35S:ARP7/Col, and p35S:AG transgenic line were obtained in this study by floral infiltration, while pSYD:SYD C1/syd-5 (Su et al., 2006) and pAGi:GUS transgenic plants were reported previously (Sieburth & Meyerowitz, 1997). Plants were grown at 22°C in a greenhouse under long-day conditions (16:8 h light: dark).

Plasmid construction

For Y2H analysis, full-length coding sequences (CDS) of *LFR* and SWI/SNF complex genes, or truncated *SYD* and *BRM* were amplified with specific primers (Table S3) from the cDNA prepared from the Col-0 Arabidopsis seedlings. The amplified fragment was digested using an appropriate restriction endonuclease, and inserted into yeast two-hybrid vectors: p*GADT7* (prey) and p*GBKT7* (bait). All construction plasmids obtained were checked via sequencing. p*GADT7-LFR* (*AD-LFR*) and p*GBKT7-SWI3B* (*BD-SWI3B*) were reported previously by the authors (Lin et al., 2018).

For the BiFC experiment, full-length CDS of *LFR*, *SYD C1*, *SWI3A/B*, *ARP4/*7, and *SWP73A/B*, with or without the stop codon were amplified via PCR using the Arabidopsis cDNA as a template. They were further cloned into pENTRY/D/SDTOPO, and these genes were introduced into pxcCFPGW or pxnYFPGW, and pcCFPxGW or pnYFPxGW by LR reactions were reported previously by the authors (Lin et al., 2018).

For the binary vectors of the transgenic complementation and genetic analyses, full-length CDS of *ARP4* and *ARP7* were amplified with specific primers (Table S3), digested using appropriate restriction endonucleases, and introduced into binary vectors p*CAMBIA2300-35S:6MYC* to generate p*35S:ARP4-6MYC* and p*35S:ARP7-6MYC*. These plasmids were transformed into Agrobacterium strain GV3101, and individually into the Col-0 to get the p*35S:ARP4-MYC* and p*35S:ARP7-MYC* lines.

Nuclear protein extracts and Western blot

Nuclear proteins were extracted from 1 g of inflorescence. Nuclear protein extraction and Western blot processes were performed as described by Lin et al. (2018), with minor modifications. Polyvinylidene fluoride membranes were probed with anti-LFR rabbit polyclonal antiserum (0.5 $\mu g \cdot ml^{-1}$) (Lin et al., 2018), 2 $\mu g \cdot ml^{-1}$ anti-SYD antibody (rabbits against the synthesized polypeptide 'EDGFRGELFDPKGR', amino acids 319 332 of SYD), 0.2 $\mu g \cdot ml^{-1}$ anti-SWI3A (both anti-SYD and anti-SWI3A antibodies were generated by Gen Script, http://www.genscript. com), 0.5 $\mu g \cdot ml^{-1}$ anti-SWI3B (Sarnowski et al., 2002), 0.2 $\mu g \cdot ml^{-1}$ anti-FLAG (Sigma, No. F3165), and 0.5 $\mu g \cdot ml^{-1}$ anti-H3 (Abcam, No. ab1791) for 2 h. Goat anti-rabbit or anti-mouse IgG secondary antibodies were used for immunodetection.

Gel filtration chromatography

Approximately 500 µg of total proteins were extracted from Arabidopsis seedlings according to a previously described process (Lin et al., 2021), with some modifications. The protein concentration should not exceed 2 mg·ml⁻¹, and the protein solution was filtered by a 0.22 µm Millipore membrane. The Superose 6 chromatography column (Superpose 6 increase 10/300, No. 71501874-EK) were analyzed with a high/low molecular weight calibration kit (Amersham) using a cleaning solution (50 mM Na₂HPO₄/NaH₂PO₄ pH7.4, 150 mM NaCl, 0.05 0.1 Triton X-100, 15 glycerol, 1 mM PMSF, Fresh add 1 Roche protease inhibitor complete) as the mobile phase before chromatography. The protein sample was placed in the injection ring after rinsing with 1 ml mobile phase. A total of 26 samples were collected at 0.5 mL intervals. After collection, each sample was added into StrataClean Resin for protein enrichment, followed by Western blot analysis with anti-FLAG antibodies (Sigma, No. F3165).

Co-immunoprecipitation co-IP) and immunoprecipitation combined with mass spectrometry IP-MS)

For co-IP experiments, 10 g fresh 14-day-old p35S:LFR-3FLAG/Ifr-1, p35S:ARP4-MYC/p35S:ARP7-MYC single and double transgenic seedlings, or inflorescence, and 30-day-old rosette leaves were ground into fine powder in liquid nitrogen, and the total protein extraction was performed using protein solution buffer (50 mM Na₂HPO₄/NaH₂PO₄, pH7.4, 150 mM NaCl, 1 Triton X-100, 15 glycerol, 1 mM PMSF and 1 protease inhibitor cocktail from Roche). The protein supernatant was filtered twice through two layers of microcloth, and incubated with 50 µl anti-FLAG Magnetic beads (Sigma, No. M8823) for 2 h at 4°C. The beads were washed three times with washing buffer (50 mM Na₂HPO₄/NaH₂PO₄, pH 7.4, 150 mM NaCl, 0.1 Triton X-100, 10 glycerol, 1 mM PMSF, and 1 protease inhibitor cocktail from Roche). Elute proteins from beads were isolated using 1 SDS at room temperature. The IP proteins were analyzed by Western blotting using anti-FLAG. anti-MYC, anti-H3 antibody, anti-LFR polyclonal antiserum, anti-SWI3A, and anti-SWI3B (Sarnowski et al., 2002).

For IP-MS, ~20 g fresh 10-day-old or wild-type seedlings were extracted using 100 µl anti-FLAG Magnetic beads (Sigma, No. M8823) for 2 h at 4°C. The beads were washed with 10 volumes of wash buffer at 4°C. Elute proteins were obtained from beads using 200 µl 1 SDS at room temperature and then boiled for 5 min at 100°C. The IP experiment was repeated across 15 independent biological replicates, and each 5 IP protein samples were mixed together to obtain IP1, IP2, and IP3 protein samples of SDS-PAGE gel. Some protein samples were subjected to western blot

analysis to make sure that LFR-FLAG proteins were enriched successfully. Lyophilized samples were dissolved in 100 ul 2 Laemmli buffer, separated by 12 1D SDS-PAGE in a largeformatted vertical electrophoresis cell, and stained with Deep Purple total protein stain. The protein bands of the IP sample or control gel were excised for in-gel trypsin digestion by grademodified trypsin (Promega, No. promega V5111). The peptide samples were lyophilized and resuspended in reversed-phase HPLC buffer (0.4 AcOH, 0.005 heptafluorobutyric anhydride in H₂O). The identities of the polypeptides present in each band were then determined by liquid chromatography tandem mass spectrometry (LC MS/MS). LC MS/MS data were acquired in a datadependent acquisition controlled by Xcalibur v.2.0 (Thermo Fisher Scientific), while spectral data were searched against the TAIR v.10 databases using Protein BioWorks v.3.3.1. LC MS/MS data of IP1, IP2, and IP3 for p35S:LFR-FLAG/Ifr-1 and WT (negative control) were presented in Table S1.

Yeast two-hybrid Y2H) assays

Y2H assays were performed as described in the Clontech Yeast Protocols Handbook. Full-length LFR and SWI/SNF genes, or truncated SYD and BRM were cloned into two vectors (pGADT7 and pGBKT7) and co-transformed into yeast strain AH109 or Y2HGold. The co-transformed colonies were chosen to grow on a selective medium that lacked leucine and tryptophan (SD/-L-W). A growth assay was then conducted, in which the physical interaction between different pairs of proteins were tested on a selective medium that lacked leucine, tryptophan, adenine, and histidine (SD/-I-W-A-H).

Bimolecular fluorescence complementation BiFC)

BiFC analysis was performed using the methods previously described in (Ou et al., 2011). The plasmids were transformed into Agrobacterium GV3101 and co-infiltrated into the leaves of N. benthamiana. After incubation for ~48 h, the fluorescent pictures were taken on LSM 710 confocal microscope (Zeiss). The GFP and DAPI signals were excited at 488 and 405 nm, and emitted at 535 nm and 460 nm. The pX-CCFP and pX-NYFP, or CCFP-pX and *NYFP*-pX empty vectors were used as negative controls.

Microarray assay and data analysis

For microarray analysis, three biological replicate RNA samples were prepared from inflorescences with 3 4 opening flowers at 38 40 days for Col-0, Ifr-2, or syd-5. RNA isolation, purification, and microarray hybridization were carried out by the CapitalBio Corporation (http://www.capitalbio.com, Beijing, China) using Affymetrix ATH1 Genome array. Arrays were scanned by Affymetrix GeneChip Scanner 3000, and image analyses were performed with Affymetrix Expression Console™. To determine the significant differentially expressed genes, Significance Analysis of Microarrays (SAM, v.3.02) was performed (Tusher et al., 2001), and Fisher's exact test was used to determine statistical significance. Genes with q value () < 5, and a fold change of mutant to wild type (|FC|) > 2 were considered significantly altered in expression. Heat map analysis was conducted using TBtools, and Gene Ontology term enrichment was conducted using Blast2GO.

RNA extraction, RT-PCR, and real-time quantitative PCR

Total RNA was extracted using the Trizol reagent (TaKaRa) from inflorescences with 3 4 opening flowers. A total of 500 ng of RNA was used for cDNA synthesis via an SYBR PrimeScriptTM RT-PCR

Kit (TaKaRa). PCR fragments were amplified using their specific primers (Table S3), analyzed via 2 agarose gel, and stained with Goldview[™] Nucleic Acid Stain. ACTIN7 was used for constitutive expression control. Real-time PCR was subsequently performed to quantify cDNA using SYBR Premix Ex Tag (TaKaRa) in a 7500 realtime PCR instrument (Applied Biosystems) by corresponding primers (Table S3). EAF4a1 was used as an internal control.

-Glucuronidase GUS) staining and fluorometric assays

GUS staining and GUS fluorometric assays were performed in accordance with (Jefferson et al., 1987). For the GUS fluorometric assays, total soluble proteins were extracted from 0.1 g inflorescences and quantified by the Bradford method according to the procedures of Jefferson et al. (1987) and Lin et al. (2018).

Chromatin immunoprecipitation ChIP) assav

The ChIP procedure was performed as reported (Yamaguchi et al., 2014). Briefly, 0.3 0.6 g of inflorescences with three to four opening flowers were crosslinked with 1 formaldehyde before being fully ground in liquid nitrogen. Chromatin was isolated using nuclei lysis buffer, and cut into approximately 500 bp DNA fragments via sonication. The chromatin suspension was incubated with 50 µl magnetic protein G beads (Invitrogen, No. 10004D) for 2 h at 4°C. Subsequently, chromatin suspension was incubated with either 5 mg of anti-FLAG antibody (Sigma, No. F3165), 5 mg of anti-GFP antibody (Abcam, No. ab290), 5 mg of anti- H3K27me3 antibody (Millipore, No. 07-473), 50 µl anti-pol II (Millipore, No. 07-352), 10 μ l anti-SYD antibody, or 2 μ l anti-LFR rabbit polyclonal antiserum (taking pre-immune serum as the control). A DNA purification kit (Qiagen, No. 28104) was used in the purification of immunoprecipitated DNA and was applied in real-time quantitative PCR as a template using the primers shown in Table S3.

MNase assay

The nuclei were isolated as described in Liu et al. (2014) from 1 g of inflorescences with 3 4 open flowers from Col-0, Ifr-2, syd-5, and Ifr-2 syd-5 plants using 50 mM Tris HCl, 5 mM CaCl₂, BSA, 20 μg·ml⁻¹ RNase A, and 1 protease inhibitor cocktail from Roche. The DNA integrity analysis was detected by 1 agarose gel, and the DNA concentration was adjusted to ~600 µg ml⁻¹, taking 200 µl as the input. The residual chromatin was digested by 200 units ml⁻¹ micrococcal nuclease (NEB, M0247S), and incubated at 37°C. Then, the digestion reaction was terminated by adding the same volume of stop buffer (0.1 M Tris HCI, 0.1 M NaCl, 50 mM EDTA, 1 SDS, and 20 μg·ml⁻¹ proteinase K) 10 min after micrococcal nuclease was added. DNA was purified under the CTAB method and resolved in a 2 agarose gel to visualize the DNA digestion patterns. The purified DNA was quantified using Qubit v.3.0. Two nanogram's DNA were used for qPCR to monitor nucleosome occupancy. The -73 site of the At4g07700 transposon was used as a sample loading control, and data analysis was performed in accordance with (Han et al., 2012). The tiled primers used for qPCR are listed in Table S3.

Chromosome conformation capture 3C)

The 3C assay was performed as described in (Guo et al., 2018), with some minor modifications. Two grams (2 g) of 14-day-old seedlings or inflorescence was cross-linked in 4 (v/v) formaldehyde at room temperature for 20 min, followed by quenching with 0.125 M glycine. The cross-linked plantlets were ground, and the nuclei were isolated and treated with buffer (10 mM phosphate buffer, pH 7.0, 0.1 M NaCl, 10 mM β-mercaptoethanol, 1 M

494 Xiaowei Lin et al.

hexylene glycol; Sigma-Aldrich), 1 protease inhibitor cocktail (Roche), and 1 mM Phenylmethanesulfonyl fluoride. Digestions were performed overnight at 37°C with 400 units of *Nla*III and 400 units of *Dpn*II. The restriction enzymes were inactivated by the addition of 1.6 SDS, and incubation at 65°C for 20 min. SDS was sequestered with 1 Triton X-100. DNA was ligated by incubation at 22°C for 5 h in a 5 ml volume using 100 units of T4 DNA ligase. Reverse cross-linking was performed via overnight treatment at 65°C. DNA was recovered after proteinase K treatment by phenol/chloroform extraction and ethanol precipitation. Relative interaction frequencies were calculated by RT-qPCR using 15 ng of DNA, while a region uncut by *Nla*III and *Dpn*II in the proximal promoter was used to normalize the DNA amount. The primers used for 3C-qPCR are listed in Table S3.

AUTHOR CONTRIBUTIONS

HZ and SC conceived the study and designed the experiments. XL prepared anti-SWI3A antibody, did the co-IP, BiFC, western blot, microarray assay, RT-qPCR, GUS staining and fluorometric assays, ChIP assay, MNase assay, 3C, phenotypic analysis. TY prepared anti-SYD antibody, did the gel filtration, IP-MS analysis, plasmid construction, YH2, RT-PCR. YG analyzed the IP-MS data. HG prepared pLFR:-LFR-FLAG/Ifr-2 transgenic line and IP-MS. SW did some RT-qPCR and 3C. DZ did some Y2H. JL and DQ contributed to some plasmid construction and RT-qPCR. QC and XL contributed to the transcriptome data analysis. LZ and JX carried out part of the 3C experiment. NY carried out some of the ChIP assay. DW contributed to the selection of target gene. HZ, XL, TY, and SC wrote this article.

FUNDING INFORMATION

This work was supported by the National Natural Science Foundation of China (NSFC 31771351, 31400240, 82105024).

ACKNOWLEDGMENTS

We thank Prof. Xigang Liu (Hebei Normal University) for providing the plasmid of p35S:AG; We thank Prof. Andrzej Jerzmanowski (Warsaw University) for providing SWI3B antibody; Prof. Ying Sun (Hebei Normal University) for providing the constructs of binary vector and suggestion in IP complex purification. We also thank Prof. Moussa Benhamed and Dr. Teddy Jegu (Institut of Plant Sciences Paris-Saclay) and Dr. Lin Guo (Hebei Normal University) for the suggestions with MNase assay; Prof. Ligeng Ma (Capital Normal University) for the suggestions on the manuscript.

CONFLICT OF INTEREST

The authors declare no competing financial interest.

DATA AVAILABILITY STATEMENT

All relevant data can be found within the manuscript and its supporting materials.

SUPPORTING INFORMATION

Additional Supporting Information may be found in the online version of this article.

- Figure S1. The procedures and stained SDS-PAGE gel for identification of LFR-containing complexes by IP-MS assay.
- Figure S2. The negative controls of Y2H assay.
- Figure S3. LFR interacts with ARP7 in Y2H assay.
- Figure S4. The negative controls of BiFC assay.
- Figure S5. Co-immunoprecipitation of LFR with SWI3A and SWI3B in different tissues.
- **Figure S6.** Microarray expression profile was used to analyze the differentially expressed genes in inflorescence tissues of *lfr-2* and *syd-5* mutants.
- Figure S7. p35S:AG partly rescues of the development defect of mutants.
- **Figure S8.** Association of LFR and SYD with the chromatin of ABCE model genes in inflorescence.
- **Figure S9.** Nucleosome occupancy at a control locus was analyzed by MNase digestion and qPCR assay.
- Figure S10. LFR and SYD regulate the formation of a gene loop at the AG gene in inflorescences.
- Figure S11. LFR and SYD regulate the formation of a gene loop at the AG gene in seedlings.
- **Figure S12.** LFR, SYD, and CLF regulate the formation of a gene loop at the *AG* gene in *Ifr-2*, *syd-5*, and *clf-29* single and double mutant seedlings.
- Figure S13. The transcript level of AG in WT, clf-29, lfr-2, and clf-29 lfr-2 mutant background.
- **Figure S14.** Association of LFR and SYD with the chromatin of *AG* in wild-type and *clf-29* seedlings.
- **Figure S15.** Phenotypes of *lfr-2* and *syd-5* single or double mutants.
- Table S1. List of peptides identified by LC MS/MS.
- Table S2. List of Ifr-2 and syd-5 inflorescence ATH1 array.
- Table S3. List of primers used in this paper.

REFERENCES

- Alvarez-Venegas, R., Pien, S., Sadder, M., Witmer, X., Grossniklaus, U. & Avramova, Z. (2003) ATX-1, an Arabidopsis homolog of trithorax, activates flower homeotic genes. *Current Biology*, 13, 627 637. Available from: https://doi.org/10.1016/s0960-9822(03)00243-4
- Archacki, R., Yatusevich, R., Buszewicz, D., Krzyczmonik, K., Patryn, J., Iwanicka-Nowicka, R. et al. (2017) Arabidopsis SWI/SNF chromatin remodeling complex binds both promoters and terminators to regulate gene expression. Nucleic Acids Research, 45, 3116 3129. Available from: https://doi.org/10.1093/nar/gkw1273
- Bezhani, S., Winter, C., Hershman, S., Wagner, J.D., Kennedy, J.F., Kwon, C.S. et al. (2007) Unique, shared, and redundant roles for the Arabidopsis SWI/SNF chromatin remodeling ATPases BRAHMA and SPLAYED. Plant Cell, 19, 403 416. Available from: https://doi.org/10.1105/tpc.106.048272
- Bowman, J.L., Drews, G.N. & Meyerowitz, E.M. (1991) Expression of the Arabidopsis floral homeotic gene AGAMOUS is restricted to specific cell types late in flower development. *Plant Cell*, 3, 749 758. Available from: https://doi.org/10.1105/tpc.3.8.7493/8/749
- Brzeski, J., Podstolski, W., Olczak, K. & Jerzmanowski, A. (1999) Identification and analysis of the Arabidopsis thaliana BSH gene, a member of the SNF5 gene family. *Nucleic Acids Research*, 27, 2393 2399. Available from: https://doi.org/10.1093/nar/27.11.2393
- Carles, C.C. & Fletcher, J.C. (2009) The SAND domain protein ULTRAPE-TALA1 acts as a trithorax group factor to regulate cell fate in plants. Genes Development, 23, 2723 2728. Available from: https://doi.org/10.1101/gad.1812609
- Cavalli, G. & Misteli, T. (2013) Functional implications of genome topology. Nature Structural Molecular Biology, 20, 290 299. Available from: https://doi.org/10.1038/nsmb.2474

- Clapier, C.R. & Cairns, B.R. (2009) The biology of chromatin remodeling complexes. Annual Review of Biochemistry, 78, 273 304. Available from: https://doi.org/10.1146/annurev.biochem.77.062706.153223
- Dennis, L. & Peacock, J. (2019) Genes directing flower development in Arabidopsis. Plant Cell, 31, 1192 1193. Available from: https://doi.org/10. 1105/tpc, 19,00276
- Diego-Martin, B., Perez-Alemany, J., Candela-Ferre, J., Corbalan-Acedo, A., Pereyra, J., Alabadi, D. et al. (2022) The TRIPLE PHD FINGERS proteins are required for SWI/SNF complex-mediated +1 nucleosome positioning and transcription start site determination in Arabidopsis, Nucleic Acids Research, 50, 10399 10417. Available from: https://doi.org/10.1093/nar/
- Farrona, S., Hurtado, L., Bowman, J.L. & Reyes, J.C. (2004) The Arabidopsis thaliana SNF2 homolog AtBRM controls shoot development and flowering. Development, 131, 4965 4975. Available from: https://doi.org/10. 1242/dev.01363
- Fu, W., Yu, Y., Shu, J., Yu, Z., Zhong, Y., Zhu, T. et al. (2023) Organization, genomic targeting, and assembly of three distinct SWI/SNF chromatin remodeling complexes in Arabidopsis, Plant Cell. 35, 2464 2483, Available from: https://doi.org/10.1093/plcell/koad111
- Guo, J., Cai, G., Li, Y.Q., Zhang, Y.X., Su, Y.N., Yuan, D.Y. et al. (2022) Comprehensive characterization of three classes of Arabidonsis SWI/SNF chromatin remodelling complexes. Nature Plants, 8, 1423 1439. Available from: https://doi.org/10.1038/s41477-022-01282-z
- Guo, L., Cao, X., Liu, Y., Li, J., Li, Y., Li, D. et al. (2018) A chromatin loop represses WUSCHEL expression in Arabidopsis. The Plant Journal, 94, 1083 1097, Available from: https://doi.org/10.1111/tpi.13921
- Han, S.K., Sang, Y., Rodrigues, A., Wu, M.F., Rodriguez, P.L. & Wagner, D. (2012) The SWI2/SNF2 chromatin remodeling ATPase BRAHMA represses abscisic acid responses in the absence of the stress stimulus in Arabidopsis. Plant Cell, 24, 4892 4906. Available from: https://doi.org/ 10.1105/tpc.112.105114
- Han, S.K., Wu, M.F., Cui, S. & Wagner, D. (2015) Roles and activities of chromatin remodeling ATPases in plants. The Plant Journal, 83, 62 77. Available from: https://doi.org/10.1111/tpj.12877
- He, S., Wu, Z., Tian, Y., Yu, Z., Yu, J., Wang, X. et al. (2020) Structure of nucleosome-bound human BAF complex. Science, 367, 875 881. Available from: https://doi.org/10.1126/science.aaz9761
- Hernandez-Garcia, J., Diego-Martin, B., Kuo, P.H., Jami-Alahmadi, Y., Vashisht, A.A., Wohlschlegel, J. et al. (2022) Comprehensive identification of SWI/SNF complex subunits underpins deep eukaryotic ancestry and reveals new plant components. Communications Biology, 5, 549. Available from: https://doi.org/10.1038/s42003-022-03490-x
- Hurtado, L., Farrona, S. & Reyes, J.C. (2006) The putative SWI/SNF complex subunit BRAHMA activates flower homeotic genes in Arabidopsis thaliana. Plant Molecular Biology, 62, 291 304. Available from: https://doi. ora/10.1007/s11103-006-9021-2
- Ito, T., Ng, K.H., Lim, T.S., Yu, H. & Meyerowitz, E.M. (2007) The homeotic protein AGAMOUS controls late stamen development by regulating a jasmonate biosynthetic gene in Arabidopsis. Plant Cell, 19, 3516 3529. Available from: https://doi.org/10.1105/tpc.107.055467
- Ito, T., Wellmer, F., Yu, H., Das, P., Ito, N., Alves-Ferreira, M. et al. (2004) The homeotic protein AGAMOUS controls microsporogenesis by regulation of SPOROCYTELESS. Nature, 430, 356 360. Available from: https:// doi.org/10.1038/nature02733
- Jaronczyk, K., Sosnowska, K., Zaborowski, A., Pupel, P., Bucholc, M., Malecka, E. et al. (2021) Bromodomain-containing subunits BRD1, BRD2, and BRD13 are required for proper functioning of SWI/SNF complexes in Arabidopsis. Plant Communications, 2, 100174. Available from: https:// doi.org/10.1016/j.xplc.2021.100174
- Jefferson, R.A., Kavanagh, T.A. & Bevan, M.W. (1987) GUS fusions: betaglucuronidase as a sensitive and versatile gene fusion marker in higher plants. The EMBO Journal, 6, 3901 3907. Available from: https://doi.org/ 10.1002/j.1460-2075.1987.tb02730.x
- Jegu, T., Latrasse, D., Delarue, M., Hirt, H., Domenichini, S., Ariel, F. et al. (2014) The BAF60 subunit of the SWI/SNF chromatin-remodeling complex directly controls the formation of a gene loop at FLOWERING LOCUS C in Arabidopsis. Plant Cell, 26, 538 551. Available from: https:// doi.org/10.1105/tpc.113.114454
- Jegu, T., Veluchamy, A., Ramirez-Prado, J.S., Rizzi-Paillet, C., Perez, M., Lhomme, A. et al. (2017) The Arabidopsis SWI/SNF protein BAF60

- mediates seedling growth control by modulating DNA accessibility. Genome Biology, 18, 114. Available from: https://doi.org/10.1186/s13059-017-1246-
- Jerzmanowski, A. (2007) SWI/SNF chromatin remodeling and linker histones in plants. Biochimica et Biophysica Acta, 1769, 330 345. Available from: https://doi.org/10.1016/j.bbaexp.2006.12.003
- Kim, J., Bordiya, Y., Kathare, P.K., Zhao, B., Zong, W., Huq, E. et al. (2021) Phytochrome B triggers light-dependent chromatin remodelling through the PRC2-associated PHD finger protein VIL1. Nature Plants, 7, 1213 1219. Available from: https://doi.org/10.1038/s41477-021-00986-v
- Krizek, B.A. & Fletcher, J.C. (2005) Molecular mechanisms of flower development: an armchair guide. Nature Reviews Genetics, 6, 688 698. Available from: https://doi.org/10.1038/nrg1675
- Lee, U.S., Bieluszewski, T., Xiao, J., Yamaguchi, A. & Wagner, D. (2022) H2A.Z contributes to trithorax activity at the AGAMOUS locus. Molecular Plant, 15, 207 210. Available from: https://doi.org/10.1016/j.molp.2022.01.
- Li, C., Gu, L., Gao, L., Chen, C., Wei, C.Q., Qiu, Q. et al. (2016) Concerted genomic targeting of H3K27 demethylase REF6 and chromatinremodeling ATPase BRM in Arabidopsis. Nature Genetics, 48, 687 693. Available from: https://doi.org/10.1038/ng.3555
- Lin, X., Gu, D., Zhao, H., Peng, Y., Zhang, G., Yuan, T. et al. (2018) LFR is functionally associated with AS2 to mediate leaf development in Arabidopsis. The Plant Journal, 95, 598 612. Available from: https://doi.org/10. 1111/tpi.13973
- Lin, X., Yuan, C., Zhu, B., Yuan, T., Li, X., Yuan, S. et al. (2021) LFR physically and genetically interacts with SWI/SNF component SWI3B to requlate leaf blade development in Arabidopsis. Frontiers in Plant Science, 12, 717649. Available from: https://doi.org/10.3389/fpls.2021.717649
- Litt, A. & Kramer, E.M. (2010) The ABC model and the diversification of floral organ identity. Seminars in Cell Developmental Biology, 21, 129 137. Available from: https://doi.org/10.1016/j.semcdb.2009.11.019
- Liu, X., Gao, L., Dinh, T.T., Shi, T., Li, D., Wang, R. et al. (2014) DNA topoisomerase I affects polycomb group protein-mediated epigenetic regulation and plant development by altering nucleosome distribution in Arabidopsis. Plant Cell, 26, 2803 2817. Available from: https://doi.org/10. 1105/tpc.114.124941
- Ma, T., Wang, S., Sun, C., Tian, J., Guo, H., Cui, S. et al. (2023) Arabidopsis LFR, a SWI/SNF complex component, interacts with ICE1 and activates ICE1 and CBF3 expression in cold acclimation. Frontiers in Plant Science. 14, 1097158. Available from: https://doi.org/10.3389/fpls.2023.1097158
- Mashtalir, N., Suzuki, H., Farrell, D.P., Sankar, A., Luo, J., Filipovski, M. et al. (2020) A structural model of the endogenous human BAF complex informs disease mechanisms. Cell, 183(802 817), e824. Available from: https://doi.org/10.1016/j.cell.2020.09.051
- Mlynarova, L., Nap, J.P. & Bisseling, T. (2007) The SWI/SNF chromatinremodeling gene AtCHR12 mediates temporary growth arrest in Arabidopsis thaliana upon perceiving environmental stress. The Plant Journal, 51, 874 885. Available from: https://doi.org/10.1111/j.1365-313X.2007.
- Nelissen, H., Eeckhout, D., Demuynck, K., Persiau, G., Walton, A., van Bel, M. et al. (2015) Dynamic changes in ANGUSTIFOLIA3 complex composition reveal a growth regulatory mechanism in the maize leaf. Plant Cell, 27, 1605 1619. Available from: https://doi.org/10.1105/tpc.15.00269
- Ogiyama, Y., Schuettengruber, B., Papadopoulos, G.L., Chang, J.M. & Cavalli, G. (2018) Polycomb-dependent chromatin looping contributes to gene silencing during drosophila development. Molecular Cell, 71(73 88), e75. Available from: https://doi.org/10.1016/j.molcel.2018.05.032
- Ou, B., Yin, K.Q., Liu, S.N., Yang, Y., Gu, T., Wing Hui, J.M. et al. (2011) A high-throughput screening system for Arabidopsis transcription factors and its application to Med25-dependent transcriptional regulation. Molecular Plant, 4, 546 555. Available from: https://doi.org/10.1093/mp/ ssr002
- Pelayo, M.A., Yamaguchi, N. & Ito, T. (2021) One factor, many systems: the floral homeotic protein AGAMOUS and its epigenetic regulatory mechanisms. Current Opinion in Plant Biology, 61, 102009.
- Ramirez-Prado, J.S. & Benhamed, M. (2021) New partners for old friends: plant SWI/SNF complexes. Molecular Plant, 14, 870 872. Available from: https://doi.org/10.1016/j.molp.2021.05.017
- Reyes, J.C. (2014) The many faces of plant SWI/SNF complex. Molecular Plant, 7, 454 458. Available from: https://doi.org/10.1093/mp/sst147

- Sacharowski, S.P., Gratkowska, D.M., Sarnowska, E.A., Kondrak, P., Jancewicz, I., Porri, A. et al. (2015) SWP73 subunits of Arabidopsis SWI/SNF chromatin remodeling complexes play distinct roles in leaf and flower development. Plant Cell, 27, 1889 1906. Available from: https://doi.org/10.1105/tpc.15.00233
- Sang, Y., Silva-Ortega, C.O., Wu, S., Yamaguchi, N., Wu, M.F., Pfluger, J. et al. (2012) Mutations in two non-canonical Arabidopsis SWI2/SNF2 chromatin remodeling ATPases cause embryogenesis and stem cell maintenance defects. The Plant Journal, 72, 1000 1014. Available from: https://doi.org/10.1111/tpj.12009
- Sarnowska, E., Gratkowska, D.M., Sacharowski, S.P., Cwiek, P., Tohge, T., Fernie, A.R. et al. (2016) The role of SWI/SNF chromatin remodeling complexes in hormone crosstalk. Trends in Plant Science, 21, 594 608. Available from: https://doi.org/10.1016/j.tplants.2016.01.017
- Sarnowski, T.J., Rios, G., Jasik, J., Swiezewski, S., Kaczanowski, S., Li, Y. et al. (2005) SWI3 subunits of putative SWI/SNF chromatin-remodeling complexes play distinct roles during Arabidopsis development. Plant Cell, 17, 2454 2472. Available from: https://doi.org/10.1105/tpc.105.031203
- Sarnowski, T.J., Swiezewski, S., Pawlikowska, K., Kaczanowski, S. & Jerzmanowski, A. (2002) AtSWI3B, an Arabidopsis homolog of SWI3, a core subunit of yeast SWI/Snf chromatin remodeling complex, interacts with FCA, a regulator of flowering time. Nucleic Acids Research, 30, 3412 3421. Available from: https://doi.org/10.1093/nar/gkf458
- Shang, J.Y. & He, X.J. (2022) Chromatin-remodeling complexes: conserved and plant-specific subunits in Arabidopsis. *Journal of Integrative Plant Biology*, 64, 499 515. Available from: https://doi.org/10.1111/jipb.13208
- Shu, J., Chen, C., Li, C., Thapa, R.K., Song, J., Xie, X. et al. (2021) Genome-wide occupancy of Arabidopsis SWI/SNF chromatin remodeler SPLAYED provides insights into its interplay with its close homolog BRAHMA and Polycomb proteins. The Plant Journal, 106, 200 213. Available from: https://doi.org/10.1111/tpi.15159
- Sieburth, L.E. & Meyerowitz, E.M. (1997) Molecular dissection of the AGA-MOUS control region shows that cis elements for spatial regulation are located intragenically. *Plant Cell*, 9, 355-365. Available from: https://doi.org/10.1105/tpc.9.3.355
- Su, Y., Kwon, C.S., Bezhani, S., Huvermann, B., Chen, C., Peragine, A. et al. (2006) The N-terminal ATPase AT-hook-containing region of the Arabidopsis chromatin-remodeling protein SPLAYED is sufficient for biological activity. The Plant Journal, 46, 685 699. Available from: https://doi.org/10.1111/j.1365-313X.2006.02734.x
- Sun, L., Cao, Y., Li, Z., Liu, Y., Yin, X., Deng, X.W. et al. (2023) Conserved H3K27me3-associated chromatin looping mediates physical interactions of gene clusters in plants. *Journal of Integrative Plant Biology*. Available from: https://doi.org/10.1111/jipb.13502
- Tusher, V.G., Tibshirani, R. & Chu, G. (2001) Significance analysis of microarrays applied to the ionizing radiation response. *Proceedings of the National Academy of Sciences of the United States of America*, 98, 5116 5121. Available from: https://doi.org/10.1073/pnas.091062498
- Vercruyssen, L., Verkest, A., Gonzalez, N., Heyndrickx, K.S., Eeckhout, D., Han, S.K. et al. (2014) ANGUSTIFOLIA3 binds to SWI/SNF chromatin remodeling complexes to regulate transcription during Arabidopsis leaf development. Plant Cell, 26, 210 229. Available from: https://doi.org/10. 1105/tpc.113.115907
- Wagner, D. (2003) Chromatin regulation of plant development. Current Opinion in Plant Biology, 6, 20 28. Available from: https://doi.org/10. 1016/s1369526602000079
- Wagner, D. & Meyerowitz, E.M. (2002) SPLAYED, a novel SWI/SNF ATPase homolog, controls reproductive development in Arabidopsis. *Current*

- Biology, 12, 85 94. Available from: https://doi.org/10.1016/s0960-9822(01) 00651-0
- Wang, Z., Yuan, T., Yuan, C., Niu, Y., Sun, D. & Cui, S. (2009) LFR, which encodes a novel nuclear-localized armadillo-repeat protein, affects multiple developmental processes in the aerial organs in Arabidopsis. *Plant Molecular Biology*, 69, 121 131. Available from: https://doi.org/10.1007/ s11103-008-9411-8
- Wellmer, F., Alves-Ferreira, M., Dubois, A., Riechmann, J.L. & Meyerowitz, E.M. (2006) Genome-wide analysis of gene expression during early Arabidopsis flower development. *PLoS Genetics*, 2, e117.
- Wu, H.W., Deng, S., Xu, H., Mao, H.Z., Liu, J., Niu, Q.W. et al. (2018) A noncoding RNA transcribed from the AGAMOUS (AG) second intron binds to CURLY LEAF and represses AG expression in leaves. The New Phytologist, 219, 1480 1491. Available from: https://doi.org/10.1111/nph. 1521
- Wu, M.F., Sang, Y., Bezhani, S., Yamaguchi, N., Han, S.K., Li, Z. et al. (2012) SWI2/SNF2 chromatin remodeling ATPases overcome polycomb repression and control floral organ identity with the LEAFY and SEPALLATA3 transcription factors. Proceedings of the National Academy of Sciences of the United States of America, 109, 3576 3581. Available from: https://doi.org/10.1073/pnas.1113409109
- Wu, M.F., Yamaguchi, N., Xiao, J., Bargmann, B., Estelle, M., Sang, Y. et al. (2015) Auxin-regulated chromatin switch directs acquisition of flower primordium founder fate. eLife, 4, e09269. Available from: https://doi.org/ 10.7554/eLife.09269
- Wu, X., Dinneny, J.R., Crawford, K.M., Rhee, Y., Citovsky, V., Zambryski, P.C. et al. (2003) Modes of intercellular transcription factor movement in the Arabidopsis apex. *Development*, 130, 3735-3745. Available from: https://doi.org/10.1242/dev.00577
- Xiao, J., Jin, R. & Wagner, D. (2017) Developmental transitions: integrating environmental cues with hormonal signaling in the chromatin landscape in plants. *Genome Biology*, 18, 88. Available from: https://doi.org/10. 1186/s13059-017-1228-9
- Xiao, J., Jin, R., Yu, X., Shen, M., Wagner, J.D., Pai, A. et al. (2017) Cis and trans determinants of epigenetic silencing by Polycomb repressive complex 2 in Arabidopsis. Nature Genetics, 49, 1546 1552. Available from: https://doi.org/10.1038/ng.3937
- Yamaguchi, N., Winter, C.M., Wu, M.F., Kwon, C.S., William, D.A. & Wagner, D. (2014) PROTOCOLS: chromatin immunoprecipitation from Arabidopsis tissues. *Arabidopsis Book*, 12, e0170. Available from: https://doi.org/10.1199/tab.0170
- Yang, T., Wang, D., Tian, G., Sun, L., Yang, M., Yin, X. et al. (2022) Chromatin remodeling complexes regulate genome architecture in Arabidopsis. Plant Cell, 34, 2638 2651. Available from: https://doi.org/10.1093/plcell/keps117
- Yanofsky, M.F., Ma, H., Bowman, J.L., Drews, G.N., Feldmann, K.A. & Meyerowitz, E.M. (1990) The protein encoded by the Arabidopsis homeotic gene agamous resembles transcription factors. *Nature*, **346**, 35-39. Available from: https://doi.org/10.1038/346035a0
- Yu, Y., Fu, W., Xu, J., Lei, Y., Song, X., Liang, Z. et al. (2021) Bromodomain-containing proteins BRD1, BRD2, and BRD13 are Core subunits of SWI/SNF complexes and are vital for their genomic targeting in Arabidopsis. Molecular Plant, S1674-2052(21), 888–904. Available from: https://doi.org/10.1016/j.molp.2021.03.018
- Yu, Y., Liang, Z., Song, X., Fu, W., Xu, J., Lei, Y. et al. (2020) BRAHMA-interacting proteins BRIP1 and BRIP2 are core subunits of Arabidopsis SWI/SNF complexes. Nature Plants, 6, 996 1007. Available from: https://doi.org/10.1038/s41477-020-0734-z